Post-hatchling cranial ontogeny in the Early Triassic diapsid reptile Proterosuchus fergusi

Ezcurra, Martin; Butler, Richard

DOI:
10.1111/joa.12300

Document Version
Peer reviewed version

Citation for published version (Harvard):
Ezcurra, M & Butler, R 2015, 'Post-hatchling cranial ontogeny in the Early Triassic diapsid reptile Proterosuchus fergusi', *Journal of Anatomy*, vol. 226, no. 5, pp. 387-402. https://doi.org/10.1111/joa.12300

Post-hatchling cranial ontogeny in the Early Triassic diapsid reptile *Proterosuchus fergusi*

Martín D. Ezcurra and Richard J. Butler

School of Geography, Earth and Environmental Sciences, University of Birmingham, Edgbaston, Birmingham B15 2TT, UK, and GeoBio-Center, Ludwig-Maximilians-Universität München, Richard-Wagner-Str. 10, D-80333 Munich, Germany

Running page heading: Ontogeny of the fossil reptile *Proterosuchus*

Number of words: 7,937 excluding tables and figure captions

Number of figures: 12

Number of tables: 3

Data archiving: Dryad

Correspondence: *Martín D. Ezcurra, School of Geography, Earth and Environmental Sciences, University of Birmingham, Edgbaston, Birmingham B15 2TT, UK. E: martindezcurra@yahoo.com.ar*

Abstract

The phylogenetic position of *Proterosuchus fergusi* (Lower Triassic of South Africa) as one of the most basal archosauriforms means that it is critically important for understanding the successful evolutionary radiation of archosaurs during the Mesozoic. The excellent sample of the species provides a unique opportunity to understand early archosauriform ontogeny. Qualitative and quantitative analyses of cranial ontogenetic variation were conducted on an ontogenetic sequence, in which the smallest individual is 37% of the size of the largest one and osteohistological evidence suggests that four of eleven collected specimens had not reached sexual maturity. Through ontogeny the skull of *Proterosuchus* became proportionally taller, the infratemporal fenestra larger, and the teeth more isodont and numerous but with smaller crowns. The sequence of somatic maturity supports relatively high growth rates during early ontogeny. The skull of juvenile specimens of *Proterosuchus* closely resembles adults of the basal archosauromorph *Prolacerta*, whereas adult specimens resemble adults of more derived archosauriforms. As a result, a plausible hypothesis is that ontogenetic modification events (e.g. heterochrony) may have been key drivers of the evolution of the general shape of the skull at the base of Archosauriformes. These changes may have contributed to the occupation of a new morphospace by the clade around the Permo-Triassic boundary.

Key words

Proterosuchidae, South Africa, Karoo Supergroup, standardised major axis regression, allometry, ontogram.

Introduction

Archosauromorpha is a major group of reptiles that includes all fossil and extant species that are more closely related to living birds and crocodilians than to lepidosaurs (Dilkes, 1998) (Fig. 1). The diversification of archosauromorphs following the Permo-Triassic mass extinction (251 Mya) is an excellent example of adaptive radiation in deep time, and has been the focus of extensive recent research (e.g. Brusatte et al. 2008; Nesbitt, 2011; Butler et al. 2011; Sookias et al. 2012; Ezcurra et al. 2014). This evolutionary radiation led to the origin of the crown-group, Archosauria, which includes the dinosaurs and crocodyliforms that dominated terrestrial ecosystems during most of the Mesozoic and that ultimately gave rise to modern birds and crocodylians.

The fossil reptile *Proterosuchus fergusi* is known from South African rock sequences that were deposited immediately after the Permo-Triassic mass extinction, and is one of the most basal known members of the key archosauromorph clade Archosauriformes (Fig. 1). This clade includes Archosauria and a number of closely related species that share several classic anatomical characteristics of archosaurs, such as the antorbital and external mandibular fenestrae (Gauthier et al. 1988). *Proterosuchus fergusi* is unique among early archosauromorphs and archosauriforms, because it is known from an extensive, highly ontogenetically variable sample of well-preserved three-dimensional skulls (Ezcurra & Butler, 2015). Moreover, the cranial morphology of *P. fergusi* is plesiomorphically similar in its general construction to basal members of other Permo-Triassic archosauromorph lineages (e.g. *Protorosaurus speneri*, *Macrocnemus bessani*, *Prolacerta broomi*, *Garjainia prima*, *Euparkeria capensis*) (Gottmann-Quesada & Sander, 2009; Ezcurra et al. 2013, 2014; Sookias & Butler, 2013; Gower et al. 2014). By contrast, other Triassic basal archosauromorphs known from extensive and ontogenetically variable samples

possess highly specialized skulls, and their ontogenetic trajectories are probably not useful models for understanding broader macroevolutionary processes (e.g. rhynchosaurids, proterochampsids: Langer et al. 2000; Trotteyn et al. 2013). As a result, an understanding of ontogenetic changes during the development of *P. fergusi* has the potential to shed light on the role of ontogenetic modification events (e.g. heterochrony) in the early evolutionary history of archosauromorphs, and the origin and diversification of archosauriforms.

Welman & Flemming (1993) conducted the first quantitative analysis of the cranial morphometrics of the South African proterosuchids, and demonstrated that all known specimens fitted well within a single ontogenetic series. The South African proterosuchid sample has improved in the last 20 years through the collection of new fossil specimens, and the taxonomy of *Proterosuchus* has been revisited and substantially revised (Ezcurra & Butler, 2015). Moreover, methodological advances over the same time interval have led to new approaches to analysing ontogeny in fossil species (e.g. ontograms: Brochu, 1992). As a result, a new, detailed study of the ontogeny of *P. fergusi* is necessary and timely. We conduct here qualitative and quantitative analyses of the ontogeny of this species and discuss the implications for the early evolution of Archosauromorpha, which ultimately resulted in the dominance of dinosaurs during the rest of the Mesozoic.

Institutional abbreviations

BP, Evolutionary Studies Institute (formerly Bernard Price Institute for Palaeontological Research), University of the Witwatersrand, Johannesburg, South Africa; BSPG, Bayerische Staatssammlung für Paläontologie und Geologie, Munich, Germany; GHG, Geological Survey, Pretoria, South Africa; NM, National Museum,

Bloemfontein, South Africa; RC, Rubidge Collection, Wellwood, Graaff-Reinet, South Africa; SAM-PK, Iziko South African Museum, Cape Town, South Africa; TM, Ditsong National Museum of Natural History (formerly Transvaal Museum), Pretoria, South Africa.

Materials and methods

Studied specimens and available ontogenetic series

The total number of fossil specimens of *P. fergusi* available for study has increased since Welman & Flemming (1993), and three additional, recently collected, fairly complete skulls are available (BP/1/4224, SAM-PK-11208, K10603). The improved sampling means that seven skulls (BP/1/3993, BSPG 1934 VIII 514, GHG 231, RC 59, 846, SAM-PK-11208, K140) are currently available from which the complete length of the skull can be directly measured (i.e. length between the anterior tip of the premaxilla and the posterior tip of the cranio-mandibular joint). Based on these more complete specimens, it is possible to estimate the skull length of four additional partial skulls with good statistical support (R^2>0.99; see Appendix 1). As a result, it is possible to use skull length directly as a standard measurement for the allometric regressions conducted here, contrasting with the use of proxies of skull size by Welman & Flemming (1993).

The neotype of *P. fergusi* proposed by Ezcurra & Butler (2015) (RC 846) and 10 referred specimens (RC 59, BP/1/3993, 4016, 4224, SAM-PK-11208, K140, K10603, BSPG-1934-VIII-514, TM 201 and GHG 231) were examined first hand (see Ezcurra & Butler, 2015). Precise stratigraphic data is lacking for specimens collected more than 50 years ago (R. Smith pers. comm. 2012), but there exists consensus that all specimens studied were collected from the *Lystrosaurus*

Assemblage Zone (earliest Triassic: Induan–early Olenekian) of South Africa (Welman, 1998). The smallest specimen available in the sample (RC 59: total skull length of 177.6 mm) has a skull length that is 37.2% of that of the largest specimen (GHG 231: total skull length of 477.0 mm) (Fig. 2). Similarly, the total body length and snout-vent length ratios between the smallest and largest sampled specimens of *P. fergusi* are estimated at between 35 and 37% (using equations described by Platt et al. [2009: dorsal cranial length versus total and snout-vent lengths] for the extant crocodile *Crocodylus moreletti* to estimate total and snout-vent lengths in the fossil species the ratios are 36.7% and 36.3%, respectively; and using an equation described by Webb & Messel [1978: total head length versus snout-vent length for the 13−60 cm size class] for the extant crocodile *Crocodylus porosus* the ratio is 35.6%). The broad size range present in the available sample suggests that it can be interpreted as a growth series and approximates the snout-vent length difference between hatchling and maximum adult size of some extant reptiles (e.g. the lepidosaur *Gambelia sila*; Germano & Williams, 2005: hatchlings are 36.4% of the adult length). However, the size range in the *P. fergusi* sample is considerably lower than the skull length and snout-vent length ranges observed between hatchling and large adult individuals of some extant crocodiles (e.g. *Crocodylus moreletii*; Pérez-Higareda et al. 1991; Barrios-Quiroz & Casas-Andreu, 2010: hatchlings are 5.6-6.1% of the adult cranial length and 4.6-5.0% of the adult snout-vent length). The substantial differences in size range between *P. fergusi* and some extant crocodiles are probably because the upper and lower limits of the size range of *P. fergusi* have not yet been sampled, but it is also possible that this difference at least partially results from differing growth strategies.

143 Most specimens of *P. fergusi* consist solely of cranial remains. By contrast,
144 osteohistological assessment of ontogenetic stage in fossil species generally requires
145 postcranial remains (usually limb bones: Hutton, 1986; Games, 1990; Woodward &
146 Moore, 1992; Chinsamy, 1993; Tucker, 1997; Erickson & Brochu, 1999; Erickson et
147 al. 2003; Erickson, 2005). As a result, osteohistological information useful to
148 determine ontogenetic stages is very limited for *P. fergusi* and currently limited to
149 two specimens (Botha-Brink & Smith, 2011). The osteohistology of hindlimb bones
150 indicates that the specimen SAM-PK-K140 (total skull length of 287.0 mm: 60.2% of
151 the maximum recorded skull length for the species) was a non-sexually mature
152 individual that was growing relatively fast at the time of its death, with fibro-lamellar
153 bone tissue and no lines of arrested growth (LAGs) (Botha-Brink & Smith, 2011). By
154 contrast, SAM-PK-11208 (total skull length of 350.0 mm: 73.4% of the maximum
155 recorded skull length for the species) possesses lamellar-zonal and parallel-fibered
156 bone tissue with secondary remodelling and multiple LAGs, suggesting that it was a
157 late sub-adult or adult individual at the time of its death (Botha-Brink & Smith, 2011).
158 Botha-Brink & Smith (2011) suggested that the dramatic change in growth observed
159 between SAM-PK-K140 and SAM-PK-11208 was because the latter specimen had
160 reached sexual maturity. Accordingly, it can be hypothesized that the largest known
161 individuals of *P. fergusi* (e.g. BSPG-1934-VIII-514, TM 201, GHG 231) had reached
162 or were close to the maximum size of the species because they are considerably larger
163 than the probably already sexually mature SAM-PK-11208. By contrast, SAM-PK-
164 K140 and smaller specimens (e.g. RC 59, BP/1/4016, 4224) are considered to be
165 juvenile individuals. In agreement with this idea, the neurocentral sutures are still
166 visible in the postaxial cervical vertebrae of SAM-PK-K140, but these sutures cannot
167 be discerned in the cervical vertebrae of SAM-PK-11208 and BSPG 1934 VIII 514.

These sutures progressively close (a closed neurocentral suture has no trace on the surface of the bone sensu Brochu [1996]) in a posterior-anterior pattern along the axial series during the ontogeny of crocodiles and, as a result, it is a useful criterion to determine ontogenetic stages (Brochu, 1996) that has been widely applied to fossil archosaurs (see Irmis, 2007). Accordingly, the available sample seems to be adequate to examine ontogenetic changes during the post-hatchling development of *P. fergusi*.

The skull reconstruction of the juvenile ontogenetic stage of *P. fergusi* is based on RC 59 and BP/1/4016 and the reconstruction for the adult ontogenetic stage is based on BSPG 1934 VIII 514, GHG 231 and RC 846 (Ezcurra & Butler, 2015) (Fig. 2).

Qualitative analysis

Examination of the growth series of *Proterosuchus fergusi* revealed variable characters within the sample that can be best explained as ontogenetic variation. Some of these characters cannot be measured or currently show discrete states (e.g. pattern of the sutures on the skull roof, appearance of a pineal fossa). As a result, these characters are discussed qualitatively.

Quantitative analysis: allometric regressions

Raw data for the allometric regressions consisted of 158 linear cranial measurements (plus skull length), the angle between the proximal and distal ends of the quadrate, and tooth counts of the tooth rows of the premaxilla, maxilla and dentary. Measurements were taken first hand with a digital calliper with a maximum deviation of 0.02 mm, but measurements were rounded to the nearest 0.1 mm. Ninety-four of the original measurements were not considered for the allometric regressions because

193 they could only be measured for three or fewer individuals (due to incomplete
194 preservation). As a result, 68 variables were retained and $\log_{10}$-transformed to fit the
195 linear power function before conducting the regression analyses (Gould, 1966).
196 One regression was calculated for each of the 68 variables using the
197 standardised major axis (SMA) regression method implemented in the package Smatr
198 version 3.2.6 for R (Warton et al. 2012; R Development Core Team, 2013). SMA
199 regression was employed instead of ordinary least squared regression because it has
200 been suggested to be the most appropriate method to study allometry in bivariate data
201 (Warton et al. 2006; Smith, 2009). Some authors have employed the first axis of a
202 principal component analysis (PCA) as proxy for body size in allometric regression
203 analyses (e.g. Fernandez Blanco et al. in press). However, PCA is not a reliable
204 method for the present data set because of the low number of variables that could be
205 measured for all or most of the specimens (PCA does not allow missing data). As a
206 result, total skull length was used as the independent variable for all SMA regressions.
207 R^2 and p-values were obtained from each SMA regression. Variables were
208 excluded from further consideration if their regression against skull length was
209 statistically non-significant. For variables with a statistically significant fit, the
210 allometric coefficient (K) (i.e. the slope of the regression) with its respective 90%
211 confidence intervals (CIs) was calculated and a statistical test (Pitman, 1939; Warton
212 et al. 2006) was conducted to determine if the slope was significantly different from 1
213 (H_0=slope not different from 1). Growth was considered isometric if the allometric
214 coefficient was not significantly different from 1. Conversely, the growth was
215 considered allometric if the allometric coefficient was significantly ($p<0.05$) or
216 marginally significantly ($0.05<p<0.10$) different from 1 (i.e. $K>1$ represents a positive
217 allometry and $K<1$ represents a negative allometry).

After conducting the SMA regressions, the distribution of the slopes (and their lower and upper limits) was studied, first using all the variables, and second separating the variables into four different groups in order to determine differential patterns in different regions of the skull. These four groups consisted of length, height and width measurements, and variables concerning tooth morphology.

Quantitative analysis: ontogram

The vast majority of specimens of *P. fergusi* are represented only by cranial remains. As a result, information that could be used to determine the relative ontogenetic stage of specimens, such as the sequence of closure of neurocentral sutures or fusion between other postcranial bones, as well as osteohistological data, is very limited. The aim of an ontogram is to show the sequence of maturity expressed by individuals relative to one another within an ontogenetic series (Brochu, 1992; Carr & Williamson, 2004; Tykoski, 2005; Carr, 2010; Frederickson & Tumarkin-Deratzian, 2014). The basic idea behind an ontogram is the same as a phylogenetic analysis, but species or supraspecific taxa are replaced with individuals and phylogenetically informative characters are replaced with ontogenetically variable characters.

An ontogram was constructed here to reconstruct the sequence of maturity of the *P. fergusi* sample. The character list is composed of 20 characters, including 12 continuous and 8 discrete and discretised characters, scored across the 11 available specimens. Maximum parsimony was chosen as the optimality criterion and the data matrix was analysed using TNT version 1.1 (Goloboff et al. 2008) using the implicit enumeration algorithm. Continuous characters (e.g. ratio between length of the premaxillary body and total length of the skull) were analysed as such, and as a result implied weights (with a concavity constant of 10) were used to mitigate the effects of

243 disproportionate character-state transformations among these characters and reduce
244 homoplasy (Goloboff et al. 2006). Zero length branches were collapsed following the
245 search.

246 The analysis was conducted rooting the trees with the smallest available
247 specimen (RC 59). A second, a posteriori analysis was conducted using a hypothetical
248 root (= artificial embryo of Carr & Williamson [2004]) scored with supposed
249 hatchling character-states to test the polarity reconstructed in the first analysis,
250 resembling the protocol followed by Carr (2010). Hatchling character-states in the
251 artificial embryo were inferred based upon the morphological trends observed among
252 small specimens. In the case of the continuous characters, the scored ratios for the
253 actual specimens seem to tend to 0 or 1 through ontogeny, respectively. As a result,
254 the extreme values 0 and 1 were used as scorings for the artificial embryo depending
255 on the tendency observed through ontogeny in the actual specimens. An artificial
256 adult (sensu Carr & Williamson, 2004) was not used in this second analysis in order
257 to decrease the number of a priori assumptions and leave the optimality criterion to
258 choose character polarities (cf. a traditional phylogenetic analysis). As an additional
259 test of the reconstructed sequence of maturity, total skull length was optimized on the
260 recovered most parsimonious trees (MPTs). Subsequently, a set of resampled trees
261 was generated using 10,000 pseudoreplications of Monte Carlo randomizations. A
262 statistical test, based on the number of values obtained from the simulated trees that
263 presented a higher consistency index than the original value, was conducted in order
264 to test if skull length fitted the MPTs significantly better than random, as is expected
265 for an ontogram. The significance coefficient (α) for this statistical analysis was at the
266 0.05 level.
267

Bivariate plots, thin plate spline analysis and general statistics

The thin plate spline (= deformation grid) analysis showing changes in skull morphology through ontogeny of *P. fergusi* was conducted following a basic geometric morphometric analysis using 21 landmarks on the reconstructed juvenile and adult stages, respectively (see Discussion). The geometric morphometric and thin plate spline analyses, bivariate plots, statistical parameters of slope distributions, and Shapiro-Wilk tests of normality distribution (α=0.05) were conducted and/or calculated in R (packages shapes version 1.1-9 and stats version 2.16.0).

Results

Qualitative analysis

The hypodigm of *P. fergusi* possesses a high degree of anatomical variation. Some of these variations cannot be explained as ontogenetic changes, such as the closure of the infratemporal fenestra by a complete lower temporal bar in some specimens and a narrower supratemporal fossa in others (Ezcurra & Butler, 2015). However, at least three anatomical variations within the hypodigm of *P. fergusi* can be explained as ontogenetic changes.

Isodont maxillary dentition

Anterior maxillary tooth crowns are distinctly distally curved and the posterior crowns are only very weakly distally curved in the smaller individuals of *P. fergusi* (RC 59, BP/1/4016) (Fig. 3A, B). By contrast, the posterior maxillary tooth crowns are also strongly curved distally in medium to large-sized individuals (SAM-PK-K10603, RC 96, GHG 231). As such, the maxillary tooth series of larger individuals is more isodont (Charig & Reig, 1970) (Fig. 3C, D).

293

294 *Skull roof sutures*

295 The fronto-nasal, fronto-parietal and parietal-interparietal sutures are strongly
296 interdigitated in small specimens, with the fronto-nasal and fronto-parietal sutures
297 showing anteroposteriorly well-developed projections (RC 59, BP/1/4016, 4224). For
298 example, the interdigitated fronto-parietal suture reaches posteriorly almost as far as
299 the anteromedial margin of the supratemporal fossae in RC 59 (Fig. 4A). By contrast,
300 in larger individuals these sutures still possess an interdigitated pattern, but have
301 projections that are considerably less well-developed anteroposteriorly (SAM-PK-
302 K10603, RC 96, BSPG 1934 VIII 514, TM 201, GHG 231) (Fig. 4B).

303

304 *Pineal fossa*

305 A pineal fossa on the dorsal surface of the frontals and parietals is only observed in
306 large individuals of *P. fergusi* (BP/1/3993, SAM-PK-K9957, SAM-PK-K10603, RC
307 96, TM 201, GHG 231) (Fig. 4B). In BPSG-1934-VIII-514 the dorsal surface of the
308 parietals is damaged and, as a result, the condition of this feature cannot be
309 determined. By contrast, in the smallest individuals of the ontogenetic series the skull
310 roof lacks a pineal fossa (RC 59, BP/1/4016, 4224) (Fig. 4A).

311

312 *Other changes*

313 The main axis of the postnarial process of the premaxilla is subparallel to the alveolar
314 margin of the bone in the smallest preserved specimen of *P. fergusi* (RC 59) (Fig. 5A,
315 B). By contrast, in all other specimens of the species the postnarial process is
316 downturned with respect to the main axis of the alveolar margin (e.g. BP/1/3993,
317 BSPG 1934 VIII 514, RC 846, SAM-PK-11208, TM 201) (Fig. 5C, D). This variation

318 can be interpreted as either non-ontogenetically related or ontogenetically related
319 because RC 59 is the only specimen with this morphotype. Nevertheless, the presence
320 of this feature in the smallest known specimen of the growth series might indicate that
321 the change in orientation of the postnarial process occurred very early in ontogeny.
322 This hypothesis could be tested with a future improved sample of early juvenile
323 specimens of *P. fergusi*.

324 Previous authors suggested that the pattern of tooth replacement of *P. fergusi*
325 changed during ontogeny (Broom, 1946). However, in agreement with Welman
326 (1998), we were unable to recognize any clear change in this feature in the
327 ontogenetic sequence. Similarly, no conclusive evidence was identified supporting the
328 hypothesis of a migration of the internal choanae to a more posterior position during
329 ontogeny (contra Welman & Flemming, 1993).

330

331 **Quantitative analysis**

332 *Allometric regressions*

333 Nineteen of the original 68 variables failed the regression test ($p>0.05$) and these
334 measurements were excluded because they do not show a significant relationship with
335 size (as measured by skull length) (e.g. width of the supratemporal fenestra, angle
336 between the proximal and distal ends of the quadrate, length and height of the external
337 mandibular fenestra, and width and height of the supraoccipital). Thirty-six variables
338 (73.5% of the variables with a significant regression) show a slope that does not
339 significantly depart from K=1 (Figs. 6A, C, 7A; Table 1). Seven measurements show
340 a positive allometric trend (14.3% of the variables with a significant regression), of
341 which four are height measurements (Figs. 6B, D, 7B, 8C; Table 1). Six variables
342 show a negative allometric trend (12.2% of the variables with a significant

343 regression), of which four are variables describing tooth morphology (Fig. 8A, B, D;
344 Table 1). The mean of all of the 49 recovered slopes is very close to K=1, because
345 most of the variables are length and width measurements, and the means of the slopes
346 of the length and width measurements are very close to K=1 (Table 2). The slopes of
347 the variables related to height measurements have a mean of around K=1.2, and those
348 related to tooth morphology have a slope of around K=0.7.
349 As a result, the length and width of the skull of *P. fergusi* show a general
350 pattern of isometric growth during ontogeny. For example, the length of the
351 premaxilla, maxilla, frontal, orbit and dentary all show isometric growth (Table 1),
352 implying that the elongated snout and enlarged premaxilla that are characteristic of
353 proterosuchids did not significantly change its proportions during ontogeny. By
354 contrast, the skull becomes proportionally taller through ontogeny, as demonstrated
355 by the positive allometric growth of the maximum height of the skull, minimum
356 height of the horizontal process of the maxilla, and heights of the orbit and
357 infratemporal fenestra. Although the absolute number of tooth positions increases
358 considerably through ontogeny for all the tooth-bearing bones (Ezcurra et al. 2013,
359 see ontogram), the ratio between tooth counts and the lengths of the bones is
360 significantly negative (Fig. 8A; Table 3). In addition, at least maxillary tooth crowns
361 become proportionally apicobasally shorter and mesiodistally narrower during
362 ontogeny.
363
364 *Ontogram*
365 The parsimony analysis yielded a single most parsimonious tree (MPT) with a fit
366 score of 0.22015, a consistency index (CI) of 0.8598 and a retention index (RI) of
367 0.8724. The tree is fully resolved and its overall topology shows a general tendency of

368 increase in body size towards its apex (Fig. 9). The smallest non-rooted specimens are
369 found as successive sister-individuals of larger specimens at the base of the tree
370 (BP/1/4016, 4224), and three of the four largest specimens are placed at the apex
371 (BSPG 1934 VIII 514, RC 846, GHG 231). The resampling statistical test found that
372 the total length of the skull fits significantly to the topology of the recovered MPT
373 ($p=0.0013$). This result is in agreement with the a priori assumption that the ontogram
374 shows a sequence of maturity (Brochu, 1992). The topology and optimization of the
375 characters on the tree were not affected when the tree was rooted with an artificial
376 embryo (i.e. RC 59 was still found as the least mature specimen). Several ambiguous
377 ontomorphies (sensu Frederickson & Tumarkin-Deratzian [2014]) are optimized
378 under accelerated transformations (ACCTRAN) for the nodes that include SAM-PK-
379 K140 and SAM-PK-K10603, and more mature individuals, respectively. These
380 ambiguous optimizations are a result of the multiple missing scorings present in
381 BP/1/4224 and SAM-PK-K140.

382 The sequence of optimization of the continuous characters on the tree is in
383 general agreement with the results of the allometric regressions. Measurements with
384 significant negative allometries show a decrease in their ratios with respect to the total
385 length of the skull through the ontogram (e.g. parietals minimum width, postorbital
386 height). Conversely, measurements with significant positive allometries show an
387 increase of their ratios through ontogeny (e.g. maxillary horizontal process height,
388 orbit height, infratemporal fenestra height, parietals maximum width, infratemporal
389 fenestra length, infratemporal fenestra height).

390 Orbit length was recovered as having an isometric growth by the allometric
391 regression analysis, but in the ontogram it optimizes with a tendency of decrease in its
392 proportional size towards more mature individuals. This result suggests negative

allometric growth for this measurement, which is in agreement with the low slope found in its SMA regression (K=0.8406). However, the relatively low regression coefficient (R^2=0.8210) and the low number of specimens that could be measured for this variable might have resulted in a negative allometric pattern being overlooked by the statistical test of isometry. The presence of a positive allometry in orbit height and a negative allometry in orbit length seems a likely explanation of the drastic modifications that occur in the shape and relative size of the orbit through the ontogeny of *P. fergusi* (Fig. 2).

The numbers of tooth positions in the premaxilla and maxilla, which are correlated with the number of tooth positions in the dentary (R^2=0.9888), increase through ontogeny, from five to nine premaxillary teeth, 20 to 30−31 maxillary teeth, and 18 to 28 dentary teeth. Other ontogenetic changes recovered by the ontogram include a downturned postnarial process of the premaxilla with respect to the alveolar margin of the bone, the appearance of a pineal fossa, more isodont maxillary tooth crowns (all strongly distally curved), less interdigitated sutures on the skull roof and completely closed neurocentral sutures in cervical vertebrae.

Discussion

Comparisons with previous studies

The increased number of specimens of *P. fergusi* available when compared with the analysis of Welman & Flemming (1993) allowed the direct use of skull length as the independent variable, constituting a clear step forward in the analysis of allometric regressions. For example, the standard measurement (i.e. the proxy for overall size) most widely used by Welman & Flemming (1993) was the minimum width between both parietals. However, our analysis has demonstrated that this variable has a

418 negative allometric trend with respect to skull length (K=0.7445, p=0.0046). Use of a
419 variable with a negative allometric trend as the independent variable will tend to
420 produce a systematic bias towards higher slope values.
421 The histogram showing the frequency of slopes recovered in this analysis
422 shows that the highest frequencies are situated around K=1 (mean=1.0683,
423 sd=0.2796, median=1.0218). As a result, the general tendency of the cranial
424 allometric regressions in the skull of *P. fergusi* is isometric (Fig. 10A; Table 2). The
425 distribution of the slopes is slightly skewed towards values higher than 1, but a
426 Shapiro-Wilk test failed to reject the null hypothesis of a normal distribution
427 (p=0.8795). The mean of the distribution of slopes recovered by Welman &
428 Flemming (1993) is 0.9093 (sd=0.4178) and the median is 0.8100. The histogram of
429 slope frequencies of Welman & Flemming (1993) is strongly skewed towards values
430 higher than 1 (Fig. 10B) and the Shapiro-Wilk test rejected the normality of the
431 distribution of these slopes (p<0.0001), in contrast to our results.
432 A second allometric analysis was conducted using the minimum width of the
433 parietals as the independent variable in order to test the possible influence of this
434 variable in the study of Welman & Flemming (1993). We employed the same
435 variables as in our initial analysis, but replaced skull length with the minimum width
436 of the parietals as the standard measurement. In this new analysis, 26 of the 49
437 regressions show a positive allometric trend, the mean of the slope values is 1.4111
438 (sd=0.3545) and the median is 1.3566. These results indicate a general positive
439 allometric trend (which is probably the result of a systematic bias), contrasting with
440 the general isometric trend recovered by our original analysis. For example, the length
441 of the dentary was found to have a significant positive allometry in this alternative
442 analysis (K=1.3566, p=0.0095), but a statistically well-supported isometric trend in

443 our original analysis. The Shapiro-Wilk test failed to reject the null hypothesis of a
444 normal distribution ($p=0.8011$), resembling the result of our original analysis but
445 contrasting with the distribution of slope values recovered by Welman & Flemming
446 (1993). A T-test found a significant difference between the slopes recovered using
447 skull length versus minimum width of the parietals as alternative independent
448 variables ($p<0.0001$). As a result, use of a different independent variable in the
449 present study partially, but not completely (e.g. it does not explain the change in the
450 shape of the distribution of the slope values), explains the differences between the
451 results of our original analysis and the results recovered by Welman & Flemming
452 (1993). Differences in specimen sampling, because of the addition of recently
453 collected specimens and the effects of the recently revised taxonomy, and
454 measurements may also contribute to the differences observed with the results of
455 Welman & Flemming (1993).
456
457 **Sequence of somatic maturity in *P. fergusi***
458 The result of the ontogram is in agreement with osteohistological data that indicates
459 that SAM-PK-11208 is a more mature individual than SAM-PK-K140 (Botha-Brink
460 & Smith, 2011) (Fig. 9). In addition, Botha-Brink & Smith (2011) proposed that
461 SAM-PK-11208 may have reached sexual maturity, whereas SAM-PK-K140 had not.
462 Following these lines of evidence, the ontogram suggests that *P. fergusi* reached
463 sexual maturity in individuals with skull lengths that were at least 60.2−73.4% of the
464 skull length of the largest individual currently known. Botha-Brink & Smith (2011)
465 proposed that *P. fergusi* possessed relatively rapid continuous growth, without LAGs,
466 prior to reaching sexual maturity, and until reaching at least 67% of the maximum
467 recorded skull length of the species. However, these authors slightly underestimated

468 the maximum recorded skull length of *P. fergusi*, and rapid continuous growth
469 continued until reaching at least 60.2% of the maximum skull length (Fig. 9) and an
470 estimated total body length of at least 60% of the maximum estimated total length of
471 the species (based on the equation of Platt et al. [2009]). If the absence of LAGs in
472 SAM-PK-K140 indicates that the specimen is younger than a year old, as has been
473 widely interpreted for other archosauriforms (Botha-Brink & Smith, 2011), this would
474 mean that the onset of sexual maturity was reached after the first year of life.

475 Similar growth timings are present in disparate diapsid reptiles, such as the
476 ornithischian dinosaur *Maiasaura peeblesorum* (an individual younger than a year old
477 was up to 50% of the maximum adult total body length; Horner et al. 2000) and the
478 varanoid lizard *Varanus niloticus* (a year old individual is around 40% of the
479 maximum snout-vent adult length; de Buffrénil & Castanet 2000).

480 Botha-Brink & Smith (2011) also suggested the possibility of extremely fast
481 growth in the basal archosauromorph *Prolacerta broomi*, also known from the earliest
482 Triassic of South Africa. They suggested that *Prol. broomi* may have reached
483 maximum size within its first year of life (assuming that growth did not temporarily
484 slow down or cease during the unfavourable growing season). However, although
485 some archosauromorphs also grew rapidly in their first year of life (see above), first
486 year growth rates are considerably lower in many other archosauromorph species (e.g.
487 15.7% of maximum total body length in extant crocodiles: Huchzermeyer, 2003;
488 15.3% of maximum femoral length in *Psittacosaurus lujiatunensis*: Erickson et al.
489 2009). As a result, rapid first year growth rates do not appear to be a general character
490 of archosauromorphs – instead, this feature appears to be rather homoplastic within
491 the group. Changes in growth strategies among archosauromorphs may have been
492 influenced by non-phylogenetic, external factors (e.g. climate, interspecific

493 competition) and it is striking that both archosauromorph species known from the
494 *Lystrosaurus* AZ of South Africa for which information is available on growth rates
495 (*Prol. broomi*, *P. fergusi*) appear to have attained more than 60% of their maximum
496 recorded size during the first year of life.

497 The result of the ontogram in combination with osteohistological evidence
498 allows the interpretation that RC 59, BP/1/4016, 4224 and SAM-PK-K140 represent
499 sexually immature (juvenile) individuals (skull length<300 mm) and SAM-PK-11208,
500 BSPG 1934 VIII 514, RC 846 and GHG 231 represent sexually mature (adult)
501 individuals (skull length≥350−444 mm) (Fig. 9). The ontogenetic stages of SAM-PK-
502 K10603, BP/1/3993 and TM 201 are ambiguous because they are bracketed by the
503 oldest immature and the youngest mature individuals. The earliest somatic changes
504 recognized within the sampled ontogenetic sequence of *P. fergusi* include a
505 downturned postnarial process of the premaxilla with respect to the alveolar margin of
506 the bone, increases in the minimum height of the maxillary horizontal process,
507 maximum height of the postorbital and maximum width of the parietals, and a
508 decrease in the minimum width of the parietals. During the somatic maturity of
509 juvenile specimens the maximum width of the parietals continued to increase and the
510 oldest recognized juvenile has six tooth positions in the premaxilla and 22 in the
511 maxilla. Several changes are recognized in the ontogenetic sequence of specimens
512 with an ambiguous ontogenetic stage, including the appearance of a more isodont
513 maxillary dentition, 7 tooth positions in the premaxilla and 27 in the maxilla, poorly
514 interdigitated skull roof sutures, pineal fossa, increases in the height of the orbit and
515 length of the infratemporal fenestra, and decreases in the length of the orbit and
516 minimum width of the parietals. Some of these changes may be correlated with the
517 onset of sexual maturity. Somatic changes in the unambiguously recognized youngest

518 sexually mature individual include the presence of 8 tooth positions in the premaxilla
519 and fully closed neurocentral sutures in the cervical vertebrae. The latest changes
520 recognized here during the ontogeny of *P. fergusi* are the presence of 9 tooth positions
521 in the premaxilla and 30 or more teeth in the maxilla, increase in the height of the
522 orbit and infratemporal fenestra, and decreases in the length of the orbit, height of the
523 postorbital, and minimum width of the parietals.
524
525 **Allometric growth patterns in *P. fergusi* and possible palaeoecological**
526 **implications**
527 The results of the allometric regressions suggest three main patterns during the
528 ontogeny of *P. fergusi*: isometric growth in the anteroposterior and transverse
529 directions; positive allometric growth in a dorsoventral direction; and a negative
530 allometric growth of the dentition. The result of the thin plate spline analysis showing
531 changes between the skull reconstruction of a juvenile and an adult individual is in
532 agreement with the results of the allometric regressions and the ontogram (Fig. 11).
533 The areas that suffered stronger shape changes are located in the orbital and temporal
534 regions. The adult thin plate spline shows relative anteroposterior and dorsoventral
535 elongations in the area occupied by the infratemporal fenestra and a relative
536 dorsoventral elongation in the area occupied by the orbit. Conversely, the area
537 occupied by the orbit shows a relative anteroposterior shortening. No landmarks were
538 placed on the tooth crowns, but a reduction in the size of the premaxillary and
539 maxillary teeth is evident in a comparison of the reconstructions of the juvenile and
540 adult skulls.
541 The changes in morphology observed between juvenile and adult individuals
542 of *P. fergusi* may have had implications for the palaeocology of the species. The

543 presence in juveniles of a dorsoventrally lower and more gracile skull, with less
544 numerous and proportionally larger teeth than in the adult forms may have resulted in
545 different prey selections between juveniles and adults. This behavioural
546 differentiation would have reduced the degree of intraspecific competition between
547 the two ontogenetic stages. This hypothesis could be tested in the future with
548 morphofunctional analyses that go beyond the scope of this paper.
549

550 **Implications for early archosauromorph evolution**

551 The role of ontogenetic modifications between ancestor-descendant species in the
552 early evolution of archosauromorphs and archosauriforms is mostly unknown because
553 of the scarce knowledge of the ontogenetic development of basal members of these
554 clades. The new information presented here for *P. fergusi* provides the most detailed
555 insight yet available into the ontogenetic development of an early archosauromorph
556 species. However, the ontogenetic development of other early archosauromorph and
557 archosauriform species remains poorly understood, greatly hampering detailed
558 analyses of ontogenetically related evolutionary processes. The ontogenetic changes
559 demonstrated here for *P. fergusi* allow us to propose some novel hypotheses about the
560 role of ontogenetic modification in the early archosauromorph radiation. These
561 hypotheses can be tested by future more complete sampling of the ontogenetic
562 trajectories of other basal archosauromorphs.

563 Juvenile specimens of *P. fergusi* possess a dorsoventrally low skull, with a
564 sub-circular orbit. This morphology closely resembles the generalised morphology
565 present in adult specimens of protorosaurs (one of the most basal archosauromorph
566 radiations) and *Prol. broomi* (Modesto & Sues, 2004; Gottman-Quesada & Sander,
567 2009) (Fig. 12). By contrast, adult specimens of *P. fergusi* possess a dorsoventrally

deeper and more massive skull, with an anteroposteriorly compressed, suboval orbit. This morphology closely resembles the generalised skull morphology of adult individuals of the more crownward archosauriforms Erythrosuchidae (e.g. *Garjainia prima*, *Erythrosuchus africanus*: Gower, 2003; Ezcurra et al. 2013) and *Euparkeria capensis* (Ewer, 1965).

In a phylogenetic context, this means that juveniles of *P. fergusi* resemble the adults of early archosauromorphs, including a species repeatedly recovered as the sister-taxon of Archosauriformes in recent phylogenetic analyses (*Prol. broomi*; Modesto & Sues, 2004; Gottman-Quesada & Sander, 2009; Ezcurra et al. 2014). By contrast, the adults of diverse groups of basal archosauriforms are generally similar to one another in overall skull construction (Fig. 12). As a result, we hypothesize that ontogenetic modification events (probably peramorphosis) may have been the main drivers in the evolution of the general shape of the skull (dorsoventral height, shape of the orbit) at the base of Archosauriformes. This hypothesis implies that the probable major heterochronic processes are the opposite of those operating in the evolution of early birds, in which the paedomorphic skull morphology of adult birds resembles that of juvenile non-avian theropods (Bhullar et al. 2012). Accordingly, ontogenetic modification events between different species may have contributed to the occupation of a new region of morphospace by early archosauriforms around the Permo-Triassic boundary. The cranial morphospace of non-archosauriform archosauromorphs was limited to gracile and low skulls, possibly adapted to preying upon smaller animals (e.g. insects and small reptiles and synapsids). Massive and dorsoventrally deep skulls are documented for the first time in the archosauromorph evolution in basal archosauriforms (e.g. adult proterosuchids, erythrosuchids and *Euparkeria*) and this cranial morphology seems to have appeared independently several times in the

593 lineage (e.g. ‘rauisuchians’, ornithosuchids, herrerasaurids; Sereno & Novas, 1993;
594 Baczko & Ezcurra, 2013; Nesbitt et al. 2013). These massive skulls probably allowed
595 the occupation of new niches, including the role of top predators in their respective
596 ecosystems.
597

598 ## Acknowledgements

599 We thank the following curators, researchers and collection managers that provided
600 access to specimens under their care for the purpose of this research: Bernhard Zipfel,
601 Bruce Rubidge, Jonah Choiniere and Fernando Abdala (BP); Markus Moser and
602 Oliver Rauhut (BSPG); Ellen de Kock (GHG); Elize Butler and Jennifer Botha-Brink
603 (NM); Sheena Kaal and Roger Smith (SAM); and Heidi Fourie (TM). We especially
604 thank Fernando Abdala for unpublished pictures of RC 846 and Bhart-Anjan Bhullar
605 for allowing us access to unpublished CT data of the same specimen. We thank Steve
606 Brusatte and Mark Webster for useful and insightful comments on a previous version
607 of this manuscript. The comments of two anonymous reviewers helped to improve the
608 overall quality of the manuscript. This work was supported by a grant of the DFG
609 Emmy Noether Programme (BU 2587/3-1 to RJB) and a Marie Curie Career
610 Integration Grant (PCIG14-GA-2013-630123 ARCHOSAUR RISE to RJB). Access
611 to the free version of TNT 1.1 was possible due to the Willi Henning Society.
612

613 ## References

614 **Baczko MB von, Ezcurra MD** (2013) Ornithosuchidae. In *Anatomy, Phylogeny and*
615 *Palaeobiology of Early Archosaurs and their Kin* (eds Nesbitt SJ, Desojo JB,
616 Irmis RB), pp. 187–202, London: Geol. Soc., Spec. Publ. 379.

617 **Barrios-Quiroz G, Casas-Andreu G** (2010) Crecimiento con diferentes dietas en
618 crías de C*rocodylus moreletii* Dumeril Bibron and Dumeril 1851 (Crocodylia:
619 Crocodylidae) en cautiverio, Tabasco, México. *Rev Latinoam Cons* **1**, 104–111.
620 **Bhullar B-AS, Marugán-Lobón J, Racimo F, et al.** (2012) Birds have
621 paedomorphic dinosaur skulls. *Nature* **487**, 223–226.
622 **Botha-Brink J, Smith RMH** (2011) Osteohistology of the Triassic
623 archosauromorphs *Prolacerta*, *Proterosuchus*, *Euparkeria*, and *Erythrosuchus*
624 from the Karoo Basin of South Africa. *J Vert Paleontol* **31**, 1238–1254.
625 **Brochu CA** (1992) *Ontogeny of the postcranium in crocodylomorph archosaurs*.
626 Unpublished M.A. thesis, Austin: The University of Texas at Austin.
627 **Brochu CA** (1996) Closure of neurocentral sutures during crocodilian ontogeny:
628 implications for maturity assessment in fossil archosaurs. *J Vert Paleontol* **16**,
629 49–62.
630 **Broom R** (1946) A new primitive proterosuchid reptile. *Ann Trans Mus* **20**, 343–346.
631 **Brusatte SP, Benton MJ, Ruta M, Lloyd GT** (2008) Superiority, competition, and
632 opportunism in the evolutionary radiation of dinosaurs. *Science* **321**, 1485–1488.
633 **Buffrénil V de, Castanet J (**2000) Age estimation by skeletochronology in the Nile
634 monitor (*Varanus niloticus*), a highly exploited species. *J Herpetol* **34**, 414–424.
635 **Butler RJ, Brusatte SL, Reich M, Nesbitt SJ, Schoch RR, Hornung JJ** (2011) The
636 sail-backed reptile *Ctenosauriscus* from the latest Early Triassic of Germany and
637 the timing and biogeography of the early archosaur radiation. *PLOS ONE* **6**,
638 e25693. doi:10.1371/journal.pone.0025693
639 **Carr TD** (2010) A taxonomic assessment of the type series of *Albertosaurus*
640 *sarcophagus* and the identity of Tyrannosauridae in the *Albertosaurus* bonebed

641 from the Horseshoe Canyon Formation (Campanian-Maastrichtian, Late
642 Cretaceous). *Can J Earth Sci* **47**, 1213–1226.
643 **Carr TD, Williamson TE** (2004) Diversity of late Maastrichtian Tyrannosauridae
644 (Dinosauria: Theropoda) from western North America. *Zool J Linn Soc* **142**, 479–
645 523.
646 **Charig AJ, Reig OA** (1970) The classification of the Proterosuchia. *Biol J Linn Soc*
647 **2**, 125–171.
648 **Chinsamy A** (1993) Bone histology and growth trajectory of the prosauropod
649 dinosaur *Massospondylus carinatus* Owen. *Mod Geol* **18**, 319−321.
650 **Dilkes DW** (1998) The Early Triassic rhynchosaur *Mesosuchus browni* and the
651 interrelationships of basal archosauromorph reptiles. *Philos Trans R Soc Lond B*
652 *Biol Sci* **353**, 501–541.
653 **Erickson GM** (2005) Assessing dinosaur growth patterns: a microscopic revolution.
654 *Trends Ecol Evol* **20**, 677–684.
655 **Erickson GM, Brochu CM** (1999) How the 'terror crocodile' grew so big. *Nature*
656 **398**, 205–206.
657 **Erickson GM, Ricqlès A de, Buffrénil V de, Molnar RE, Bayless MK** (2003)
658 Vermiform bones and the evolution of gigantism in *Megalania* – how a reptilian
659 fox became a lion. *J Vert Paleontol* **23**, 966–970.
660 **Erickson GM, Makovicky PJ, Inouye BD, Zhuo C, Gao K** (2009) A life table for
661 *Psittacosaurus lujiatunensis*: initial insights into ornithischian dinosaur
662 population biology. *Anat Rec* **292**, 1514–1521.
663 **Ewer RF** (1965) The anatomy of the thecodont reptile *Euparkeria capensis* Broom.
664 *Philos Trans R Soc Lond B* **751**, 379–435.

665 **Ezcurra MD, Butler RJ** (2015) Taxonomy of the proterosuchid archosauriforms
666 (Diapsida: Archosauromorpha) from the earliest Triassic of South Africa, and
667 implications for the early archosauriform radiation. *Palaeontol* **58**, 141–170.
668 **Ezcurra MD, Butler RJ, Gower DJ** (2013) 'Proterosuchia': the origin and early
669 history of Archosauriformes. In *Anatomy, Phylogeny and Palaeobiology of Early*
670 *Archosaurs and their Kin* (eds Nesbitt SJ, Desojo JB, Irmis RB), pp. 9–33,
671 London: Geol. Soc., Spec. Publ. 379.
672 **Ezcurra MD, Scheyer TM, Butler RJ** (2014) The origin and early evolution of
673 Sauria: reassessing the Permian saurian fossil record and the timing of the
674 crocodile-lizard divergence. *PLOS ONE* **9**, e89165.
675 doi:10.1371/journal.pone.0089165
676 **Fernández Blanco MV, Bona P, Olivares AI, Desojo JB** (in press) Ontogenetic
677 variation in the skulls of *Caiman*: the case of *Caiman latirostris* and *Caiman*
678 *yacare* (Alligatoridae, Caimaninae). *Herpetol J*.
679 **Frederickson JA, Tumarkin-Deratzian AR** (2014) Craniofacial ontogeny in
680 *Centrosaurus apertus*. *PeerJ* **2**, e252.
681 **Games I** (1990) Growth curves for the Nile crocodile as estimated by
682 skeletochronology. *Crocodiles*, pp. 111–121, Proceedings of the 10th Working
683 Meeting of the Crocodile Specialist Group, IUCN, Volume 1, Switzerland: The
684 World Conservation Union Gland.
685 **Gauthier JA, Kluge AG, Rowe T** (1988) Amniote phylogeny and the importance of
686 fossils. *Cladistics* **4**, 105–209.
687 **Germano D, Williams DF** (2005) Population ecology of blunt-nosed leopard lizards
688 in high elevation foothill habitat. *J Herpetol* **39**, 1–18.

689 **Goloboff PA, Mattoni C, Quinteros YS** (2006) Continuous characters analyzed as
690 such. *Cladistics* **22**, 589–601.
691 **Goloboff PA, Farris JS, Nixon KC** (2008) TNT, a free program for phylogenetic
692 analysis. *Cladistics* **24**, 774–786.
693 **Gottmann-Quesada A, Sander PM** (2009) A redescription of the early
694 archosauromorph *Protorosaurus spenseri* Meyer, 1832 and its phylogenetic
695 relationships. *Palaeontographica Abt A* **287**, 123–220.
696 **Gould SJ** (1966) Allometry and size in ontogeny and phylogeny. *Biol Rev* **41**, 587–
697 640.
698 **Gower DJ** (2003) Osteology of the early archosaurian reptile *Erythrosuchus*
699 *africanus* Broom. *Ann S Afr Mus* **110**, 1–84.
700 **Gower DJ, Hancox PJ, Botha-Brink J, Sennikov AG, Butler RJ (2014)** A new
701 species of *Garjainia* Ochev, 1958 (Diapsida: Archosauriformes:
702 Erythrosuchidae) from the Early Triassic of South Africa. *PLOS ONE* **9**,
703 e111154.
704 **Gradstein FM, Ogg JG, Schmitz MD, Ogg G** (2012) *The geologic time scale 2012*.
705 Boston: Elsevier, 144 p.
706 **Horner JR, Ricqlés A de, Padian K** (2000) Long bone histology of the hadrosaurid
707 dinosaur *Maiasaurua pebblesorum*: growth dynamics and physiology based on an
708 ontogenetic series of skeletal elements. *J Vert Paleontol* **20**, 115–129.
709 **Huchzermeyer FW** (2003) *Crocodiles: biology, husbandry and diseases*. London:
710 CABI Publishing, 352 p.
711 **Hutton JM** (1986) Age determination of living Nile crocodiles from the cortical
712 stratification of bone. *Copeia* **1986**, 332–341.

713 **Irmis RB** (2007) Axial skeleton ontogeny in the Parasuchia (Archosauria:
714 Pseudosuchia) and its implications for ontogenetic determination in archosaurs. *J*
715 *Vert Paleontol* **27**, 350–361.
716 **Langer MC, Ferigolo J, Schultz CL** (2000) Heterochrony and tooth evolution in
717 hyperodapedontine rhynchosaurs (Reptilia, Diapsida). *Lethaia* **33**, 119–128.
718 **Modesto SP, Sues H-D** (2004) The skull of the Early Triassic archosauromorph
719 reptile *Prolacerta broomi* and its phylogenetic significance. *Zool J Linn Soc* **140**,
720 335–351.
721 **Nesbitt SJ** (2011) The early evolution of archosaurs: relationships and the origin of
722 major clades. *Bull Am Mus Nat Hist* **352**, 1–292.
723 **Nesbitt SJ, Brusatte SL, Desojo JB, et al.** (2013) Rauisuchia. In *Anatomy,*
724 *Phylogeny and Palaeobiology of Early Archosaurs and their Kin* (eds Nesbitt SJ,
725 Desojo JB, Irmis RB), pp. 241–274, London: Geol. Soc., Spec. Publ. 379.
726 **Pérez-Higareda G, Rangel-Rangel A, Smith HA** (1991) Maximum sizes of
727 Morelet's and American crocodiles. *Bull Maryland Herpetol Soc* **27**, 34–37.
728 **Platt SG, Rainwater TR, Thorbjarnarson JB, Finger AG, Anderson TA,**
729 **McMurry ST** (2009) Size estimation, morphometrics, sex ratio, sexual size
730 dimorphism, and biomass of Morelet's crocodile in northern Belize. *Carib J Sci*
731 **45**, 80–93.
732 **Pitman ETG** (1939) A note on normal correlation. *Biometrika* **31**, 9–12.
733 **R Development Core Team** (2013) *R: a language and environment for statistical*
734 *computing*. Vienna: R Foundation for Statistical Computing. ISBN 3–900051–
735 07–0, available at http://www.R-project.org/.
736 **Sereno PC, Novas FE** (1993) The skull and neck of the basal theropod
737 *Herrerasaurus ischigualastensis*. *J Vert Paleontol* **13**, 451–476.

738 **Smith RJ** (2009) Use and misuse of the reduced major axis for line-fitting. *Am J Phys*
739 *Anthropol* **140**, 476–486.
740 **Sookias RB, Butler RJ** (2013) Euparkeriidae. In *Anatomy, Phylogeny and*
741 *Palaeobiology of Early Archosaurs and their Kin* (eds Nesbitt SJ, Desojo JB,
742 Irmis RB), pp. 35–48, London: Geol. Soc., Spec. Publ. 379.
743 **Sookias RB**, **Butler RJ, Benson RBJ** (2012) Rise of dinosaurs reveals major body
744 size transitions are driven by passive processes of trait evolution. *Proc R Soc B*
745 **279**, 2180–2187.
746 **Tykoski RS** (2005) *Osteology, ontogeny, and relationships of the coelophysoid*
747 *theropods*. PhD Thesis, Austin: Univ. Texas at Austin.
748 **Trotteyn MJ, Arcucci AB, Raugust T** (2013) Proterochampsia: an endemic
749 archosauriform clade from South America. In *Anatomy, Phylogeny and*
750 *Palaeobiology of Early Archosaurs and their Kin* (eds Nesbitt SJ, Desojo JB,
751 Irmis RB), pp. 59–90, London: Geol. Soc., Spec. Publ. 379.
752 **Tucker AD** (1997) Validation of skeletochronology to determine age of freshwater
753 crocodiles (*Crocodylus johnstoni*). *Mar Freshwater Res* **48**, 343–351.
754 **Warton DI, Wright IJ, Falster DS, Westoby M** (2006) Bivariate linefitting methods
755 for allometry. *Biol Rev* **81**, 259–291.
756 **Warton DI, Wright IJ, Falster DS, Westoby M** (2012) SMATR 3 – an R package
757 for estimation and inference about allometric lines. *Met Ecol Evol* **2012**, 257–
758 259.
759 **Webb GJW, Messel H** (1978) Morphometric Analysis of *Crocodylus porosus* from
760 the North Coast of Arnhem Land, Northern Australia. *Aust J Zool* **26**, 1−27.
761 **Welman J** (1998) The taxonomy of the South African proterosuchids (Reptilia,
762 Archosauromorpha). *J Vert Paleontol* **18**, 340–347.

763 **Welman J, Flemming AF** (1993) Statistical analysis of the skulls of Triassic
764 proterosuchids (Reptilia, Archosauromorpha) from South Africa. *Palaeontol Afr*
765 **30**, 113–123.
766 **Woodward AR, Moore CT** (1992) *Alligator Age Determination*. Florida Game and
767 Fresh Water Fish Commission Bureau of Wildlife Research, Final Report 7563.
768

Supplementary material

Data S1

Total skull length estimations.

The lengths of the infratemporal fenestra and dentary were the variables with the highest R^2 values, and, as a result, were used to estimate total skull length for four specimens. Power function regressions were chosen over linear regression or other models because they were the models that best explained the data set.

BP/1/4016, 4224: estimation based on a power function regression between skull length and infratemporal fenestra length ($y=0.0189x^{1.4484}$, $R^2=0.9965$, $p<0.0001$).

SAM-PK-K10603 and TM 201: estimation based on an exponential regression between skull length and dentary length ($y=59.682^{e0.0033x}$, $R^2=0.9925$, $p<0.0001$).

Data S2

Character list for the data matrix of the ontogram. Characters 1−12 are continuous characters and were scored as the ratio between the measurement and the total length of the skull.

1. Premaxilla, body height. CONTINUOUS.
2. Skull, snout minimum width. CONTINUOUS.
3. Maxilla, minimum height of the horizontal process. CONTINUOUS.
4. Maxilla, tooth crowns length at base. CONTINUOUS.
5. Jugal, height of anterior process. CONTINUOUS.
6. Orbit, length. CONTINUOUS.
7. Orbit, height. CONTINUOUS.
8. Postorbital, height. CONTINUOUS.
9. Infratemporal fenestra, length. CONTINUOUS.

10. Infratemporal fenestra, height. CONTINUOUS.
11. Parietal, maximum width of both parietals. CONTINUOUS.
12. Parietal, minimum width of both parietals. CONTINUOUS.
13. Premaxilla, orientation of postnarial process with respect to alveolar margin: parallel (0); downturned (1).
14. Premaxilla, number of tooth positions: five (0); six (1); seven (2); eight (3); nine (4). ORDERED.
15. Maxilla, number of tooth positions: 20 (0); 22 (1); 27 (2); 30 (3); 31 (4). ORDERED. The number of dentary teeth was not included because it is strongly correlated with the number of maxillary teeth in an isometric growth pattern (K=1.0415) (R^2=0.9888).
16. Maxilla, curvature of tooth crowns: posterior tooth crowns poorly distally curved (0); isodont, all tooth crowns strongly distally curved (1).
17. Skull, sutures of skull roof: strongly interdigitated (0); poorly interdigitated (1).
18. Parietal, pineal fossa: absent (0); present (1).
19. Cervical vertebrae, neurocentral sutures: open, still visible (0); completely closed, no trace of suture (1). A closed suture has no trace of the suture on the surface of the bone (Brochu, 1996).
20. Hindlimb, long bone tissues: fibro-lamellar (0); lamellar-zonal and parallel-fibered (1).

Data S3

TNT file of the data matrix analyzed in this paper.

```
nstates cont;
xread 'Data saved from TNT'
20 11
&[cont]
```

```
RC_59           0.034 0.121 0.038 0.023 0.036   ?    ?   0.175   ?    ?   0.156 0.122
BP_1_4224         ?    ?    ?    ?    ?   0.146   ?   0.167 0.215 0.155 0.267 0.113
BP_1_4016       0.036 0.098 0.052 0.019 0.037 0.129 0.121 0.160 0.220 0.154 0.230
0.108
SAM_PK_K140     0.053 0.119 0.054 0.020 0.044   ?    ?    ?    ?    ?   0.277   ?
SAM_PK_11208    0.050   ?   0.060 0.015 0.030   ?   0.139   ?   0.263 0.135   ?
0.107
BP_1_3993       0.046 0.096 0.063 0.019 0.042 0.123 0.152   ?   0.278   ?   0.202
0.099
SAM_PK_K10603     ?   0.102 0.048 0.013 0.055 0.117   ?   0.152 0.225   ?   0.279
0.092
RC_96           0.038 0.101 0.057 0.014 0.055 0.116 0.165 0.146 0.273 0.187 0.271
0.087
BSPG_1934_VIII_514  0.039 0.117 0.068 0.017 0.048 0.147 0.191 0.161 0.293 0.166
?   0.105
TM_201          0.038 0.097 0.052 0.013 0.036   ?    ?    ?    ?    ?    ?   0.091
GHG_231         0.044 0.098 0.064 0.013 0.031 0.103 0.222 0.141 0.302 0.220 0.282
0.092
&[num]
RC_59          000000??
BP_1_4224      ????00??
BP_1_4016      1?0000??
SAM_PK_K140    111???00
SAM_PK_11208   13210?11
BP_1_3993      113?11[01]?
SAM_PK_K10603  ??2111??
RC_96          1441111?
BSPG_1934_VIII_514 142?1?1?
TM_201         12??11??
GHG_231        143111??
;

Ccode
  +[/1  0     +[/1  1     +[/1  2     +[/1  3     +[/1  4
  +[/1  5     +[/1  6     +[/1  7     +[/1  8     +[/1  9
  +[/1  10    +[/1  11    ([/1  12    +[/1  13    +[/1  14
  ([/1  15    ([/1  16    ([/1  17      ([/1  18      ([/1    19    ;
piwe=10;
p/;
```

Data S4

Scorings for the hypothetical root.

```
Root    01010101000100000000
```

868 **Data S5**

869 Excel file that includes the raw measurements used for the quantitative analyses
870 (sheet 1), results of the SMA regressions excluding measurements with a N≤3 and
871 non-significant regressions (sheet 2), and results of the SMA regressions using the
872 minimum width of the parietals as independent variable (sheet 3).

873

Figure captions

Fig. 1. Simplified time calibrated tree showing the phylogenetic relationships among basal archosauromorphs. Phylogenetic relationships based on Gottman-Quesada & Sander (2009) for *Protorosaurus* and Ezcurra et al. (2014) for the other taxa. The asterisk next to Dinosauria indicates that also included within this branch are pterosaurs and non-dinosaur dinosauromorphs. Geological timescale after Gradstein et al. (2012). Abbreviations: Ani., Anisian; Cap., Capitanian; Car., Carnian; Cha., Changhsingian; Ind., Induan; Lad., Ladinian; Nor., Norian; Ole., Olenekian; Rha., Rhaetian; Roa., Roadian; Wor., Wordian; Wuc., Wuchiapingian.

Fig. 2. Cranial reconstructions of early juvenile and late adult individuals of the proterosuchid archosauriform *Proterosuchus fergusi*. The difference in size between the two skulls represents the size range of the ontogenetic sequence available in the present study. Scale bar equals 10 cm.

Fig. 3. Juvenile (A, B: BP/1/4016, reversed) and adult (C, D: SAM-PK-11208, reversed) skulls of *Proterosuchus fergusi* in lateral view, showing the changes in number, shape and size of maxillary tooth crowns during ontogeny. Scale bars equal 5 cm.

Fig. 4. Orbital and temporal regions of skulls of a juvenile (A: RC 59) and a medium-sized (B: SAM-PK-K10603) specimen in dorsal views. Fronto-nasal, fronto-parietal, frontal-frontal and parietal-parietal sutures, and the pineal fossa are highlighted with lines. Scale bars equal 2 cm.

899 **Fig. 5.** Anterior half of the snout of a juvenile (A, B: RC 59) and an adult (C, D: RC
900 846, neotype, reversed) of *Proterosuchus fergusi*. Lines show the changes in
901 orientation of the postnarial process of the premaxilla with respect to the alveolar
902 margin of the bone during ontogeny. Scale bars equal 2 cm.
903
904 **Fig. 6.** Bivariate plots showing isometric (A, C) and positive allometric (B, D) trends.
905 Dotted lines show the limits of the 90% confidence intervals and a line with a slope
906 equal to 1, respectively.
907
908 **Fig. 7.** Bivariate plots showing the possible negative allometric trend of (A) the length
909 of the orbit (A) and the positive allometric trend of the height of the orbit (B). Dotted
910 lines show the limits of the 90% confidence intervals and a line with a slope equal to
911 1, respectively.
912
913 **Fig. 8.** Bivariate plots showing negative (A, B, D) and positive (C) allometric trends.
914 Dotted lines show the limits of the 90% confidence intervals and a line with a slope
915 equal to 1, respectively.
916
917 **Fig. 9.** Single recovered most parsimonious ontogram showing the sequence of
918 somatic maturity of the available ontogenetic sequence of *Proterosuchus fergusi*.
919 Ontogenetic changes indicated with a black box are unambiguously optimized
920 characters (synontomorphies) and changes indicated with a white box are characters
921 optimized under an ACCTRAN optimization (possible ontomorphies). Upper thin-
922 section shows the bone microstructure of the probable sexually mature SAM-PK-

11208 and the lower thin-section shows the bone microstructure of the probably sexually immature SAM-PK-K140 (taken from Botha-Brink & Smith, 2011).

Fig. 10. Histograms showing the distribution of slopes recovered in the present SMA regressions (A) and the analysis of Welman & Flemming (1993) (B). The line in (A) represents a normal distribution adjusted to the data set.

Fig. 11. Position of the 21 landmarks (red dots) used for the basic geometric morphometric analysis (juvenile smaller skull on the upper left corner of the figure) and results of the thin plate spline analysis for the juvenile (left) and adult (right).

Fig. 12. Simplified phylogenetic relationships in the non-archosauriform archosauromorph to archosauriform transition showing the possible direction of heterochronic changes that contributed to the evolution of overall skull shape. Note the similarities between the juvenile skull of *Proterosuchus fergusi* and the adult of *Prolacerta broomi*, and the adult of *Proterosuchus fergusi* and an adult erythrosuchid (based on *Garjainia prima*). Scale bars equal 5 cm.

941 # Tables

942 **Table 1.** Results of the SMA regressions using total skull length as the independent
943 variable. Abbreviations: (+), marginally significant positive allometry; (-), marginally
944 significant negative allometry; +, positive allometry; -, negative allometry; =,
945 isometry; CI, confidence interval; N, size of the variable.

Measurement	N	R^2	p-value (regression-test)	Slope	Lower limit (90% CI)	Upper limit (90% CI)	p-value (isometry-test)	Trend
Skull maximum height	5	0.9013	0.0136	1.5614	1.0312	2.3642	0.0848	(+)
Length anterior to antorbital fenestra	8	0.9627	<0.0001	1.0390	0.8920	1.2102	0.6445	=
Postorbital region maximum width	6	0.7119	0.0371	1.2538	0.7272	2.1619	0.4430	=
Premaxillary body length	7	0.9094	0.0008	1.2279	0.9392	1.6053	0.1850	=
Premaxillary body height	9	0.8714	0.0002	1.2245	0.9498	1.5786	0.1761	=
Number of premaxillary teeth	8	0.6498	0.0156	0.6983	0.4436	1.0994	0.1798	=
Largest premaxillary tooth length at base	7	0.7902	0.0074	1.1434	0.7650	1.7088	0.5408	=
Snout minimum width	9	0.9256	<0.0001	0.8868	0.7303	1.0766	0.2806	=
Maxilla length	8	0.9610	<0.0001	1.1000	0.9411	1.2856	0.2811	=
Maxilla horizontal process minimum height	10	0.9339	<0.0001	1.4498	1.2254	1.7154	0.0031	+
Maxilla length anterior to antorbtial fenestra	9	0.9560	<0.0001	1.0918	0.9401	1.2581	0.3036	=
Number of maxillary teeth	9	0.8386	0.0005	0.5323	0.4008	0.7070	0.0030	-
Largest maxillary tooth height	9	0.6910	0.0054	0.6598	0.4475	0.9727	0.0810	(-)
Largest maxillary tooth length at base	10	0.6201	0.0068	0.6045	0.4073	0.8972	0.0426	-
Antorbital fenestra length	6	0.9679	0.0004	0.9721	0.8041	1.1753	0.7682	=
Lacrimal length	4	0.9275	0.0369	0.9799	0.5764	1.6659	0.9249	=
Lacrimal height	6	0.7111	0.0349	1.3518	0.7834	2.3323	0.3184	=
Jugal anterior process height	10	0.7504	0.0012	1.3242	0.9589	1.8288	0.1458	=
Orbit length	7	0.8210	0.0049	0.8406	0.5790	1.2200	0.3986	=
Orbit height	6	0.9567	0.0007	1.8453	1.4808	2.2995	0.0033	+
Frontal length	8	0.9512	<0.0001	0.9001	0.7562	1.0714	0.2864	=
Frontals minimum width	9	0.7344	0.0032	0.9030	0.6293	1.2958	0.6162	=
Postfrontal oblique length	5	0.8219	0.0338	0.7680	0.4450	1.3256	0.3532	=
Postorbital length	7	0.8586	0.0026	1.4765	1.0586	2.0593	0.0634	(+)
Postorbital height	7	0.9860	<0.0001	0.8436	0.7586	0.9382	0.0231	-
Squamosal length	6	0.7033	0.0370	0.9523	0.5482	1.6541	0.8662	=
Squamosal height	8	0.9206	0.0002	1.2089	0.9686	1.5088	0.1480	=
Squamosal ventral process height	8	0.8810	0.0005	1.2891	0.9838	1.6891	0.1180	=
Squamosal ventral process base length	8	0.8310	0.0016	0.8916	0.6470	1.2287	0.5191	=
Infratemporal fenestra length	8	0.9611	<0.0001	1.4242	1.2187	1.6642	0.0042	+
Infratemporal fenestra height	6	0.9092	0.0032	1.3923	1.0152	1.9094	0.0888	(+)
Supratemporal fenestra length	10	0.8230	0.0002	1.1224	0.8541	1.4750	0.4588	=
Supratemporal fossa width	11	0.7965	0.0012	1.2118	0.8820	1.6649	0.2942	=
Quadrate height	5	0.8144	0.0360	1.2864	0.7376	2.2434	0.3814	=
Parietal length	10	0.8314	0.0002	1.0100	0.7736	1.3188	0.9468	=
Parietals maximum width	8	0.8912	0.0004	1.4396	1.1113	1.8648	0.0326	+
Parietals minimum width	10	0.9528	<0.0001	0.7445	0.6458	0.8584	0.0046	-
Width between paroccipital processes	6	0.7940	0.0171	1.3823	0.8668	2.2043	0.2202	=

Ectopterygoid width	5	0.8044	0.0391	1.1266	0.6374	1.9912	0.6717	=
Lower jaw length	7	0.9743	<0.0001	0.9830	0.8512	1.1352	0.8212	=
Dentary length	10	0.9915	<0.0001	1.0180	0.9582	1.0814	0.5981	=
Dentary anterior height	10	0.8966	<0.0001	0.8986	0.7285	1.1083	0.3734	=
Number of dentary teeth	6	0.7152	0.0338	0.4524	0.2631	0.7778	0.0300	-
Surangular height	9	0.6858	0.0058	0.9917	0.6706	1.4666	0.9697	=
Angular length	5	0.9576	0.0037	0.9604	0.7287	1.2660	0.7566	=
Angular height	8	0.7804	0.0036	0.9398	0.6533	1.3520	0.7566	=
Retroarticular process length	6	0.8086	0.0147	1.0272	0.6544	1.6125	0.9081	=
Retroarticular process width	5	0.9641	0.0029	1.0218	0.7922	1.3180	0.8560	=
Retroarticular process height	6	0.7650	0.0226	0.8948	0.5448	1.4697	0.6699	=

946

947

948 **Table 2.** Statistical parameters of the distribution of slopes and their upper and lower

949 limits. Abbreviations: N, size of the variable; sd=standard deviation.

950

Group	N	Mean	Upper limit mean	Lower limit mean	Median	Upper limit median	Lower limit median
All variables	49	1.0683 (sd=0.2796)	1.4840 (sd=0.4317)	0.7838 (sd=0.2367)	1.0218	1.4670	0.7650
Length	19	1.0413 (sd=0.17778)	1.3850 (sd=0.2603)	0.7982 (sd=0.1945)	1.0100	1.2860	0.8041
Height	15	1.2335 (sd=0.2811)	1.7203 (sd=0.4441)	0.8994 (sd=0.2421)	1.2864	1.6891	0.9498
Width	9	1.1078 (sd=0.2367)	1.6040 (sd=0.4879)	0.7803 (sd=0.1558)	1.1266	1.6649	0.7303
Teeth	6	0.6818 (sd=0.2428)	1.0272 (sd=0.3618)	0.4546 (sd=0.1663)	0.6318	0.9349	0.4254

951

952

953 **Table 3.** Results of the SMA regressions using the respective tooth-bearing bone

954 lengths as independent variables. Abbreviations: -, negative allometry; CI, confidence

955 interval; N, size of the variable.

Measurement	N	R^2	p-value (regression-test)	Slope	Lower limit (90% CI)	Upper limit (90% CI)	p-value (isometry-test)	Trend
Premaxillary tooth count	7	0.7015	0.0186	0.5390	0.3354	0.8662	0.0186	-
Maxillary tooth count	8	0.9022	0.0003	0.4923	0.3620	0.6696	0.0009	-
Dentary tooth count	6	0.6808	0.0432	0.4505	0.2546	0.7972	0.0351	-

956

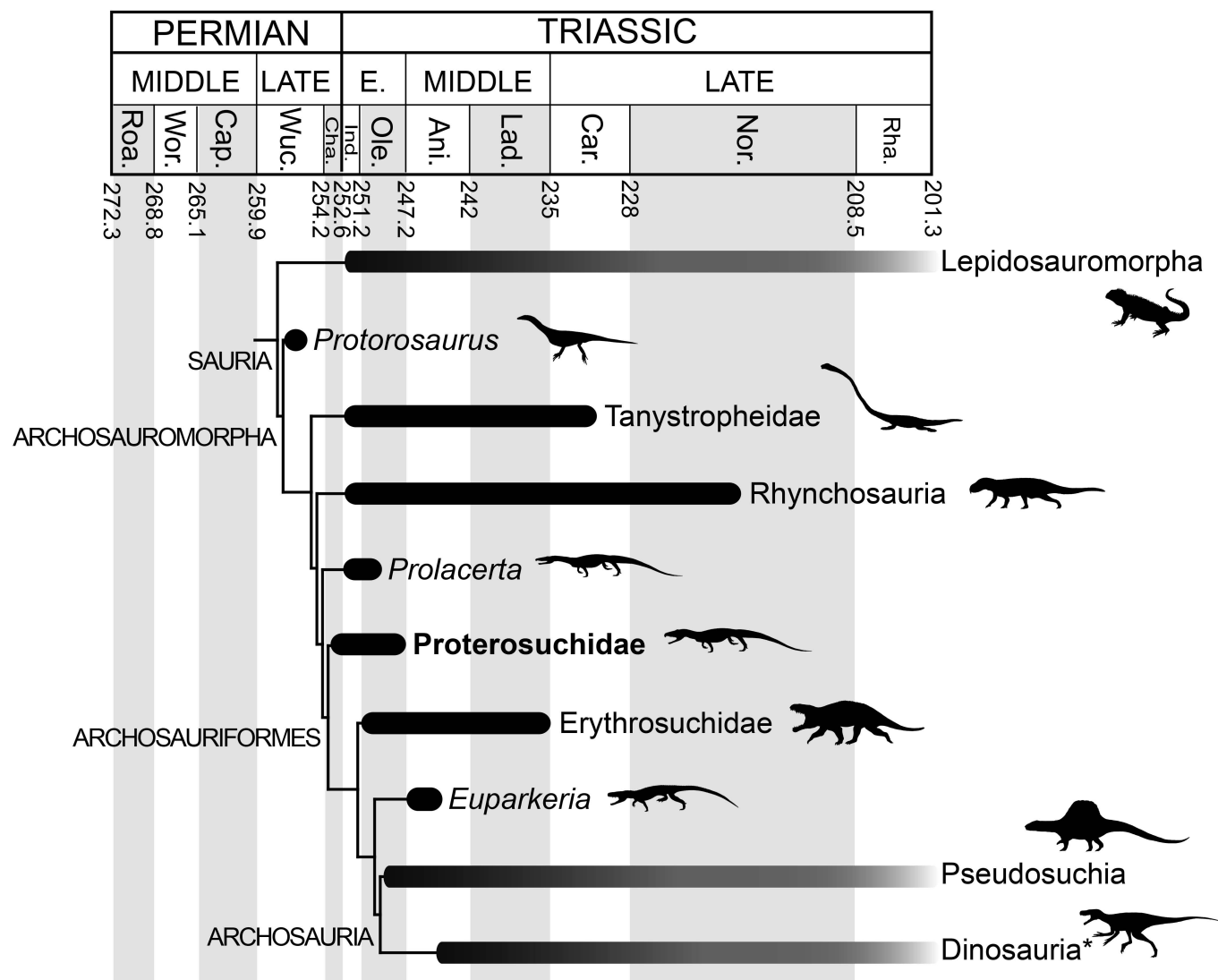
PERMIAN
TRIASSIC
MIDDLE
LATE
E.
MIDDLE
LATE
Roa.
Wor.
Cap.
Wuc.
Ind.
Cha.
Ole.
Ani.
Lad.
Car.
Nor.
Rha.
272.3
268.8
265.1
259.9
254.2
252.6
251.2
247.2
242
235
228
208.5
201.3
Lepidosauromorpha
Protorosaurus
SAURIA
Tanystropheidae
ARCHOSAUROMORPHA
Rhynchosauria
Prolacerta
Proterosuchidae
Erythrosuchidae
ARCHOSAURIFORMES
Euparkeria
Pseudosuchia
ARCHOSAURIA
Dinosauria*

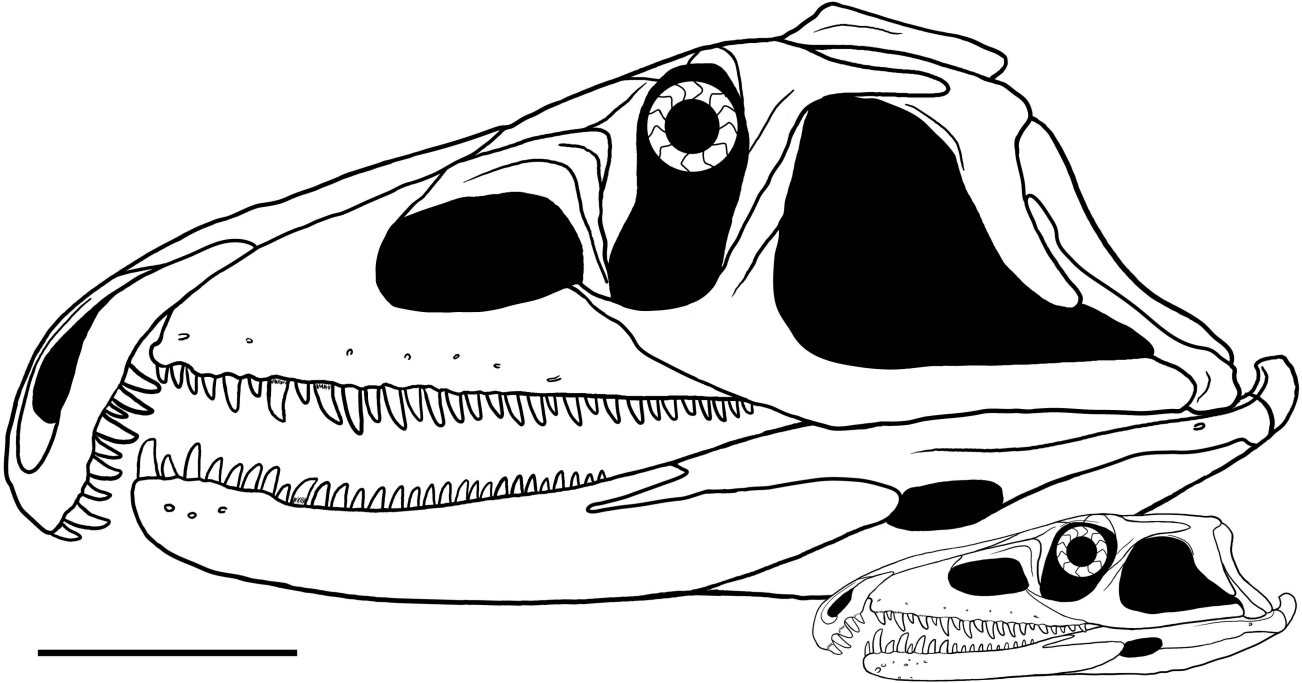

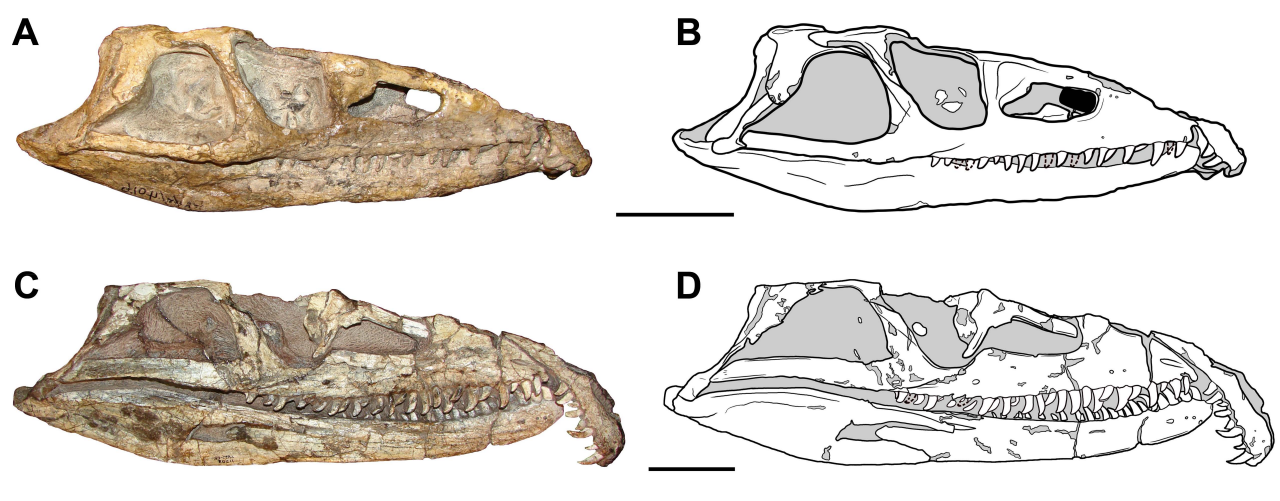
A
B
C
D

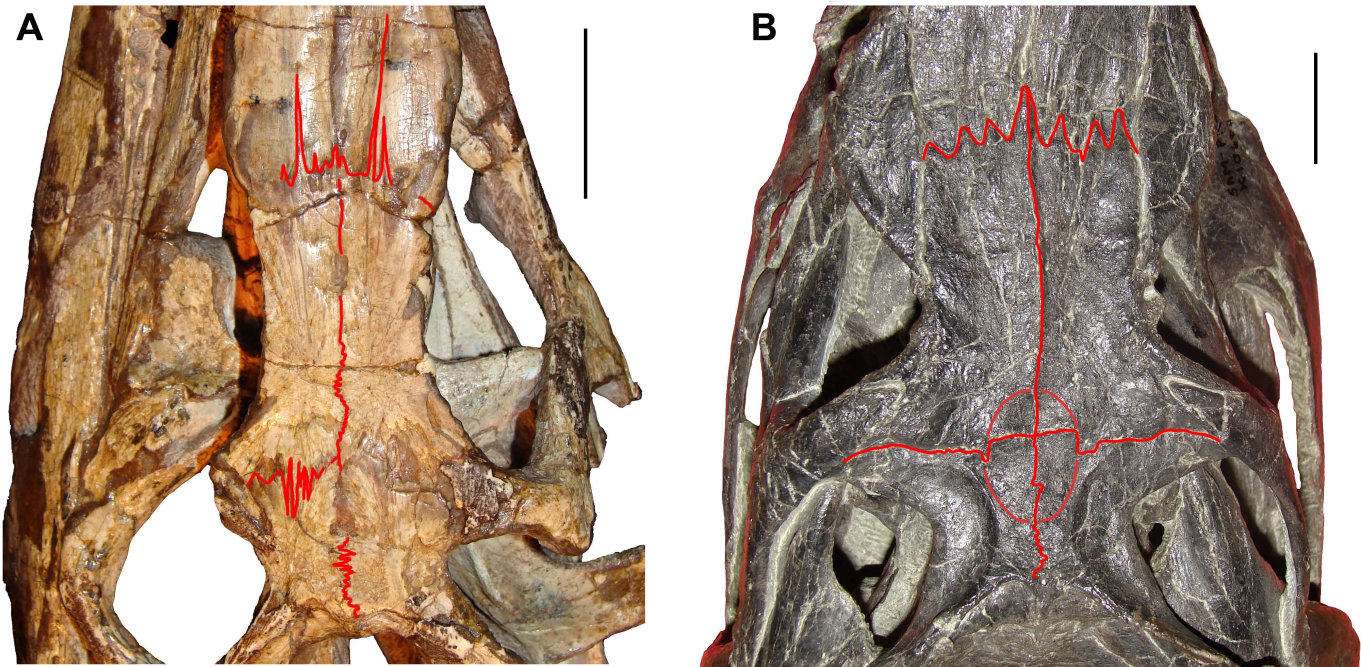
A
B

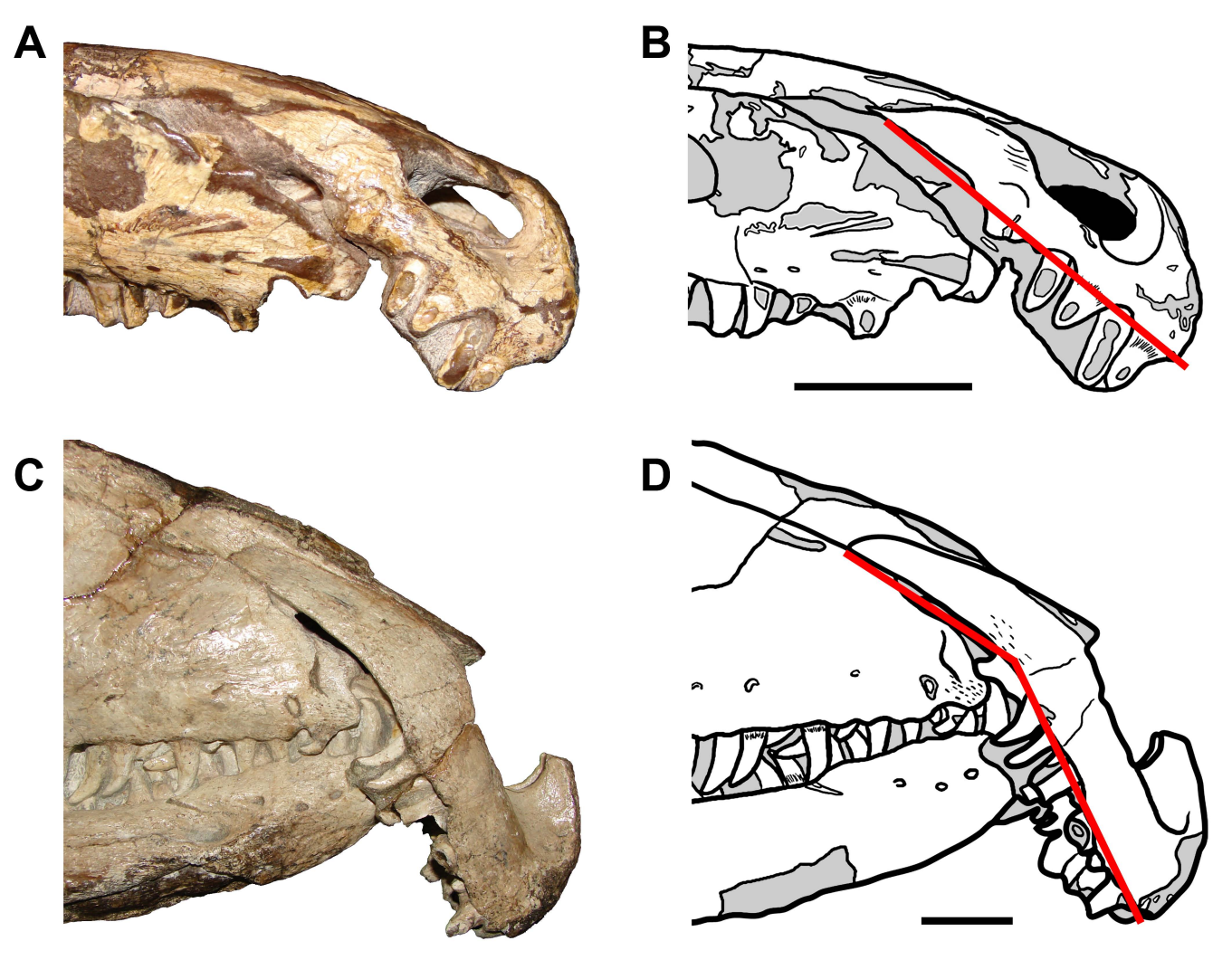
A
B
C
D

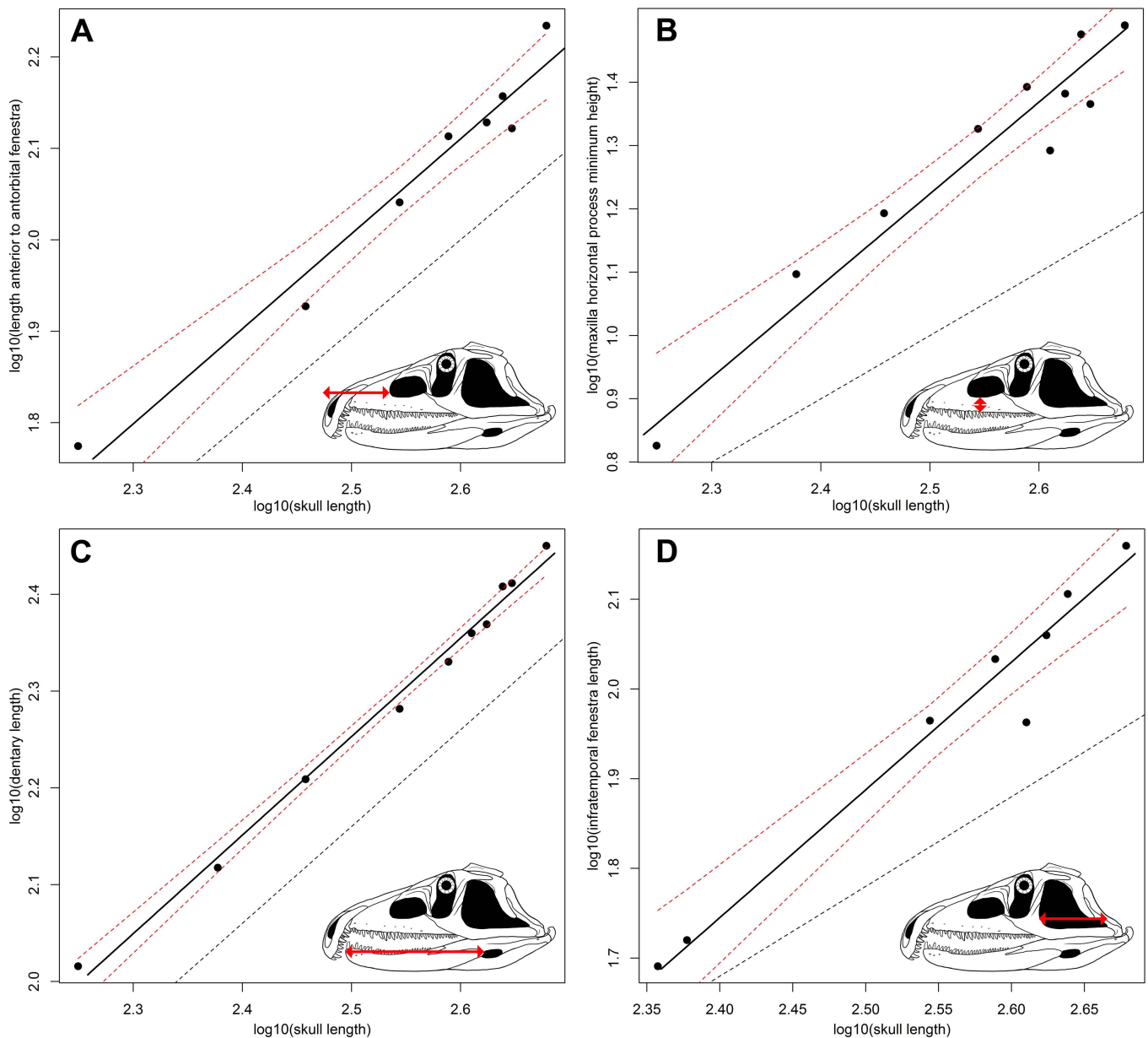
A
log10(length anterior to antorbital fenestra)
log10(skull length)
B
log10(maxilla horizontal process minimum height)
log10(skull length)
C
log10(dentary length)
log10(skull length)
D
log10(infratemporal fenestra length)
log10(skull length)

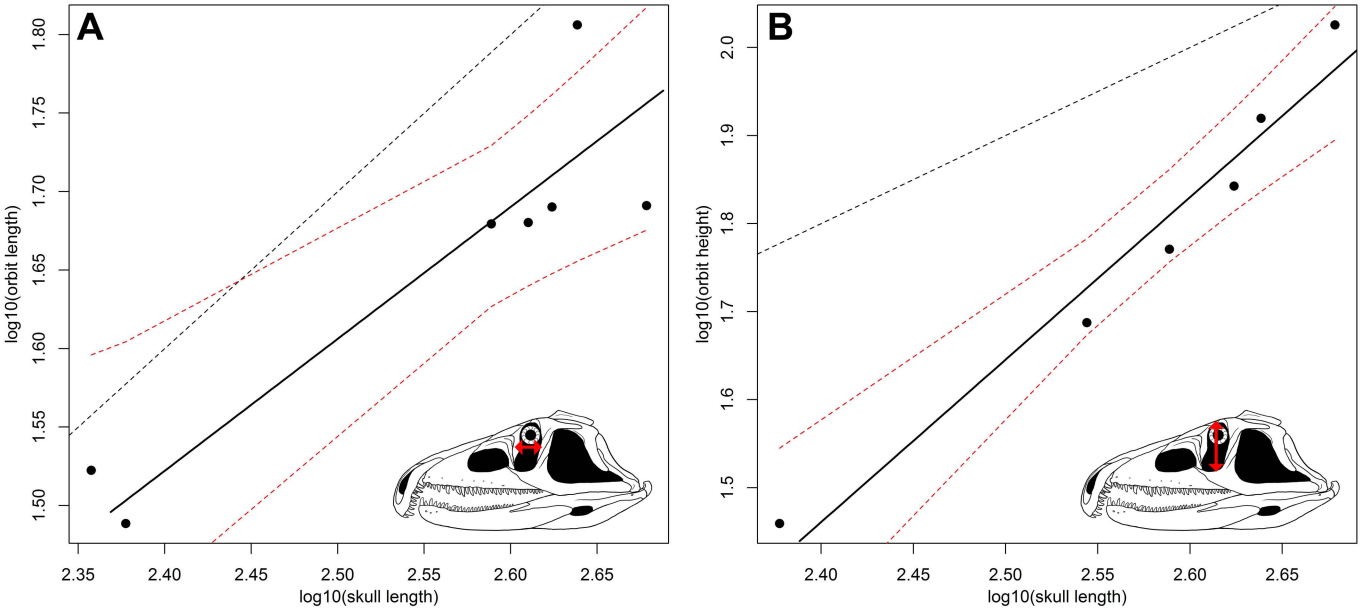
A
log10(orbit length)
1.50
1.55
1.60
1.65
1.70
1.75
1.80
2.35
2.40
2.45
2.50
2.55
2.60
2.65
log10(skull length)
B
log10(orbit height)
1.5
1.6
1.7
1.8
1.9
2.0
2.40
2.45
2.50
2.55
2.60
2.65
log10(skull length)

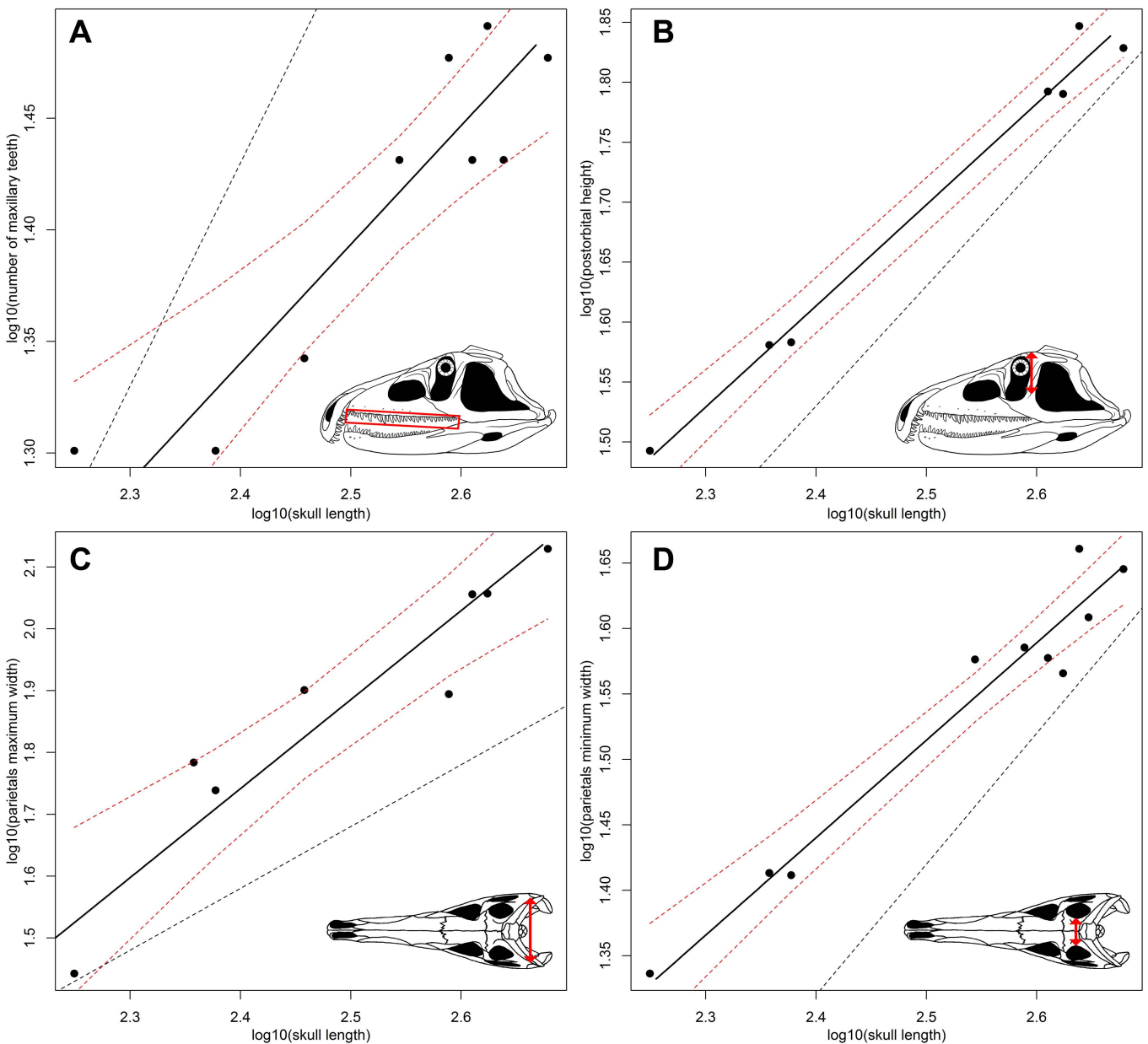
A
log10(number of maxillary teeth)
1.30
1.35
1.40
1.45
2.3
2.4
2.5
2.6
log10(skull length)
B
log10(postorbital height)
1.50
1.55
1.60
1.65
1.70
1.75
1.80
1.85
2.3
2.4
2.5
2.6
log10(skull length)
C
log10(parietals maximum width)
1.5
1.6
1.7
1.8
1.9
2.0
2.1
2.3
2.4
2.5
2.6
log10(skull length)
D
log10(parietals minimum width)
1.35
1.40
1.45
1.50
1.55
1.60
1.65
2.3
2.4
2.5
2.6
log10(skull length)

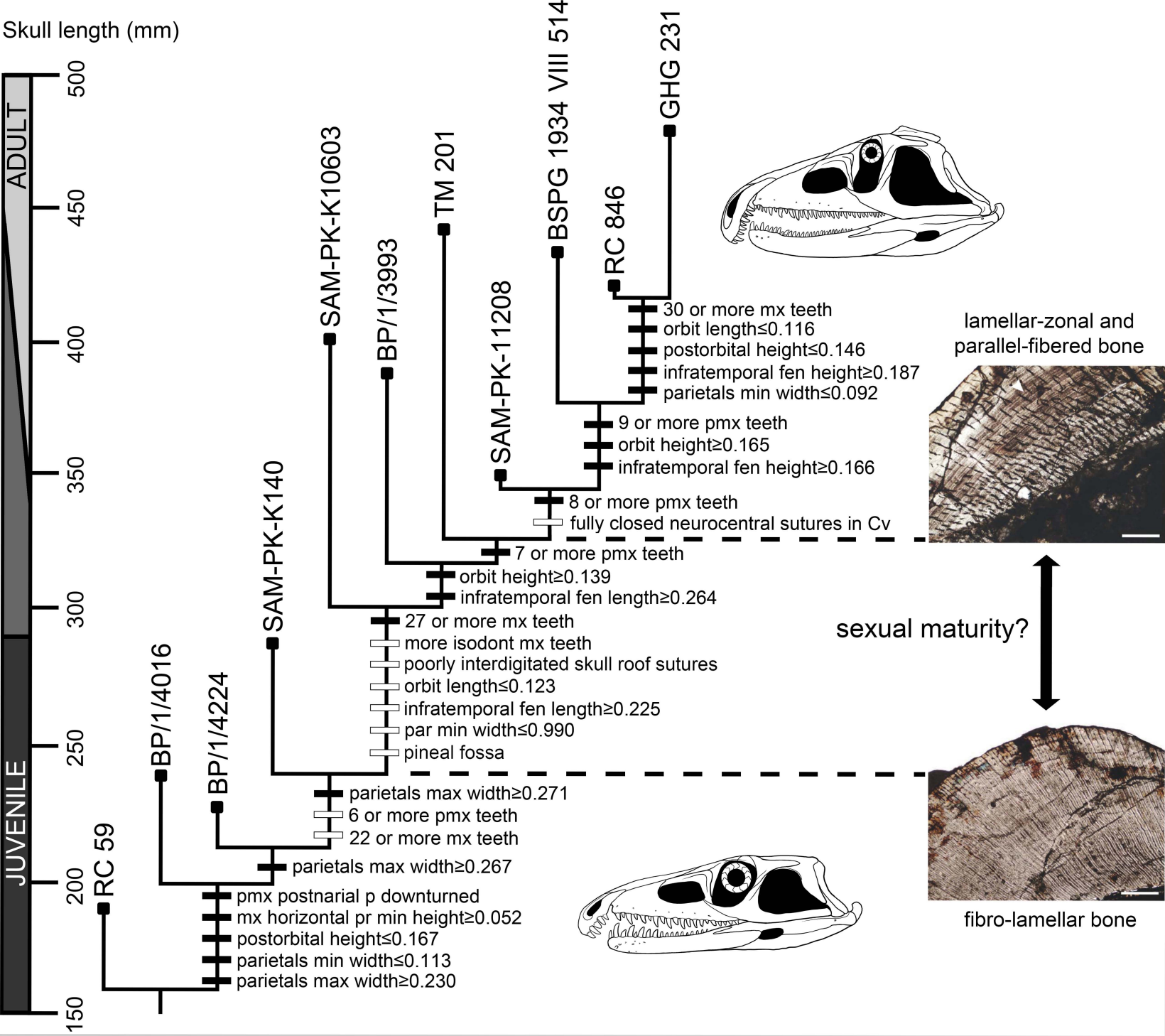
Skull length (mm)
500
450
400
350
300
250
200
150
ADULT
JUVENILE
GHG 231
BSPG 1934 VIII 514
RC 846
TM 201
BP/1/3993
SAM-PK-K10603
SAM-PK-11208
SAM-PK-K140
BP/1/4016
BP/1/4224
RC 59
30 or more mx teeth
orbit length≤0.116
postorbital height≤0.146
infratemporal fen height≥0.187
parietals min width≤0.092
9 or more pmx teeth
orbit height≥0.165
infratemporal fen height≥0.166
8 or more pmx teeth
fully closed neurocentral sutures in Cv
7 or more pmx teeth
orbit height≥0.139
infratemporal fen length≥0.264
27 or more mx teeth
more isodont mx teeth
poorly interdigitated skull roof sutures
orbit length≤0.123
infratemporal fen length≥0.225
par min width≤0.990
pineal fossa
parietals max width≥0.271
6 or more pmx teeth
22 or more mx teeth
parietals max width≥0.267
pmx postnarial p downturned
mx horizontal pr min height≥0.052
postorbital height≤0.167
parietals min width≤0.113
parietals max width≥0.230
lamellar-zonal and
parallel-fibered bone
sexual maturity?
fibro-lamellar bone

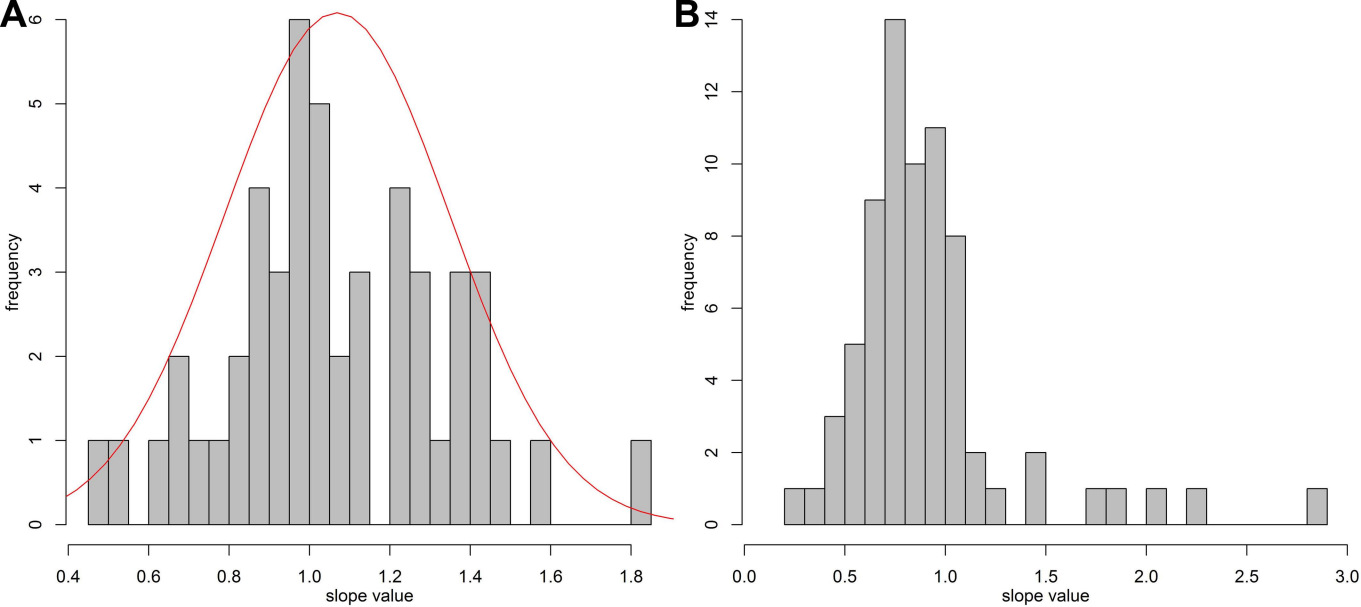
A
frequency
0
1
2
3
4
5
6
0.4
0.6
0.8
1.0
1.2
1.4
1.6
1.8
slope value
B
frequency
0
2
4
6
8
10
12
14
0.0
0.5
1.0
1.5
2.0
2.5
3.0
slope value

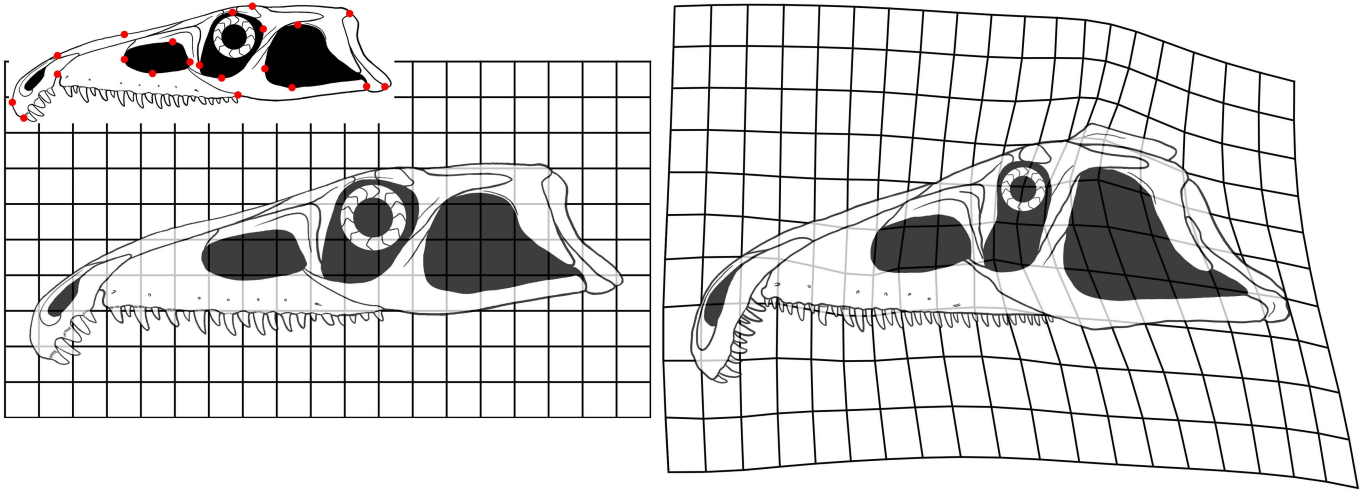

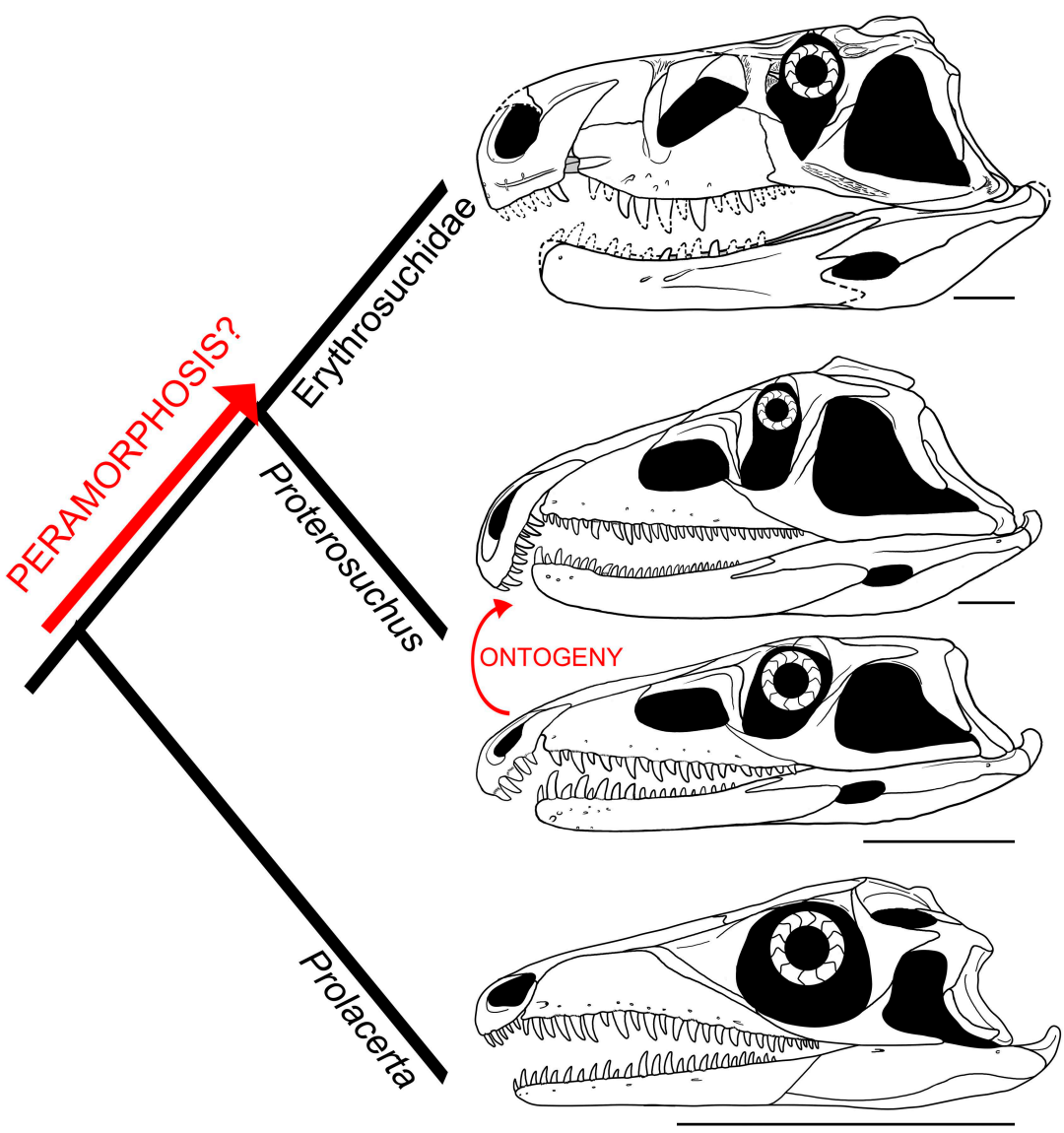
PERAMORPHOSIS?
Erythrosuchidae
Proterosuchus
Prolacerta
ONTOGENY